Introduction to Topological Quantum Materials

Prof. Pramod Kumar
Spintronics and Magnetic Materials Laboratory
Department of Applied Sciences,
Indian Institute of Information Technology Allahabad

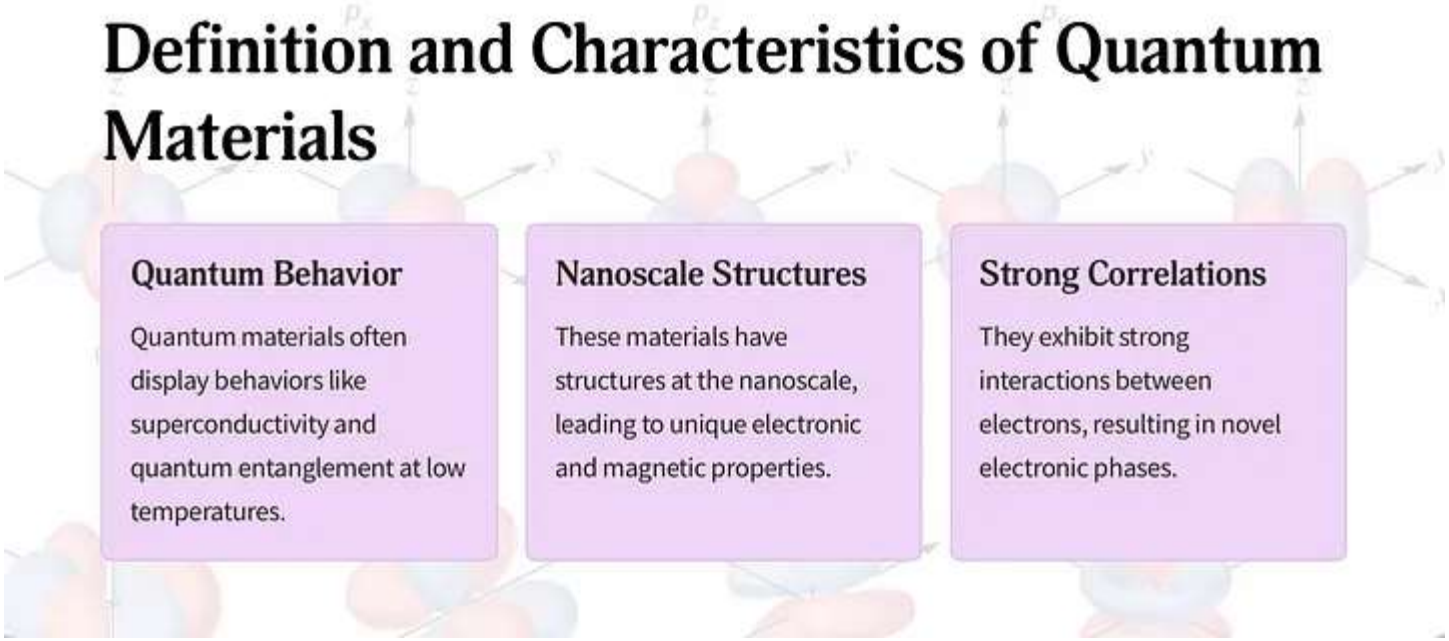

1.Emergent Quantum Phenomena:

•Quantum materials exhibit emergent quantum phenomena that arise from the collective behavior of electrons or atoms within the material.

•These phenomena can include high-temperature superconductivity, unconventional magnetism, fractional quantum Hall effects, and topological order.

2. Strong Correlations:

•Many quantum materials are characterized by strong electron-electron interactions, leading to correlated electronic states and nontrivial electronic structures.

•Strong correlations can give rise to phenomena such as Mott insulators, heavy fermions, and spin liquids, where the behavior of electrons deviates significantly from that predicted by simple band theory.

3. Topological Properties:

•Some quantum materials exhibit topological properties, where the arrangement of electronic states is robust against local perturbations and defects.

•Examples of topological materials include topological insulators, topological semimetals, and topological superconductors, which host protected surface or edge states with unique electronic properties.

4. Quantum Phase Transitions:

•Quantum materials can undergo quantum phase transitions at absolute zero temperature, driven by quantum fluctuations rather than thermal fluctuations.

•These transitions can result in the emergence of exotic phases of matter, such as quantum spin liquids, quantum critical points, and non-Fermi liquid behavior.

5. Superconductivity and Superfluidity:

•Superconductivity and superfluidity are quantum phenomena where materials exhibit zero resistance to electrical current or zero viscosity to fluid flow, respectively.

•Quantum materials can display conventional superconductivity, as well as unconventional forms such as high-temperature superconductivity and

6. Manipulable Quantum States:

•Quantum materials provide platforms for controlling and manipulating quantum states of matter, making them promising candidates for applications in quantum information processing and quantum technologies.

•Examples include materials with controllable spin, charge, and orbital degrees of freedom, as well as materials engineered for quantum computing and quantum sensing applications.

Examples of quantum materials include:

•High-temperature superconductors like cuprates and iron-based superconductors.

•Topological insulators such as bismuth telluride and mercury telluride.

•Strongly correlated electron systems like the high-temperature superconductor yttrium barium copper oxide (YBCO) and the heavy fermion compound cerium hexaboride (CeB6).

•Quantum magnets like spin liquids and frustrated magnets.

•Artificially engineered quantum systems such as quantum dots, quantum wells, and nanowires.

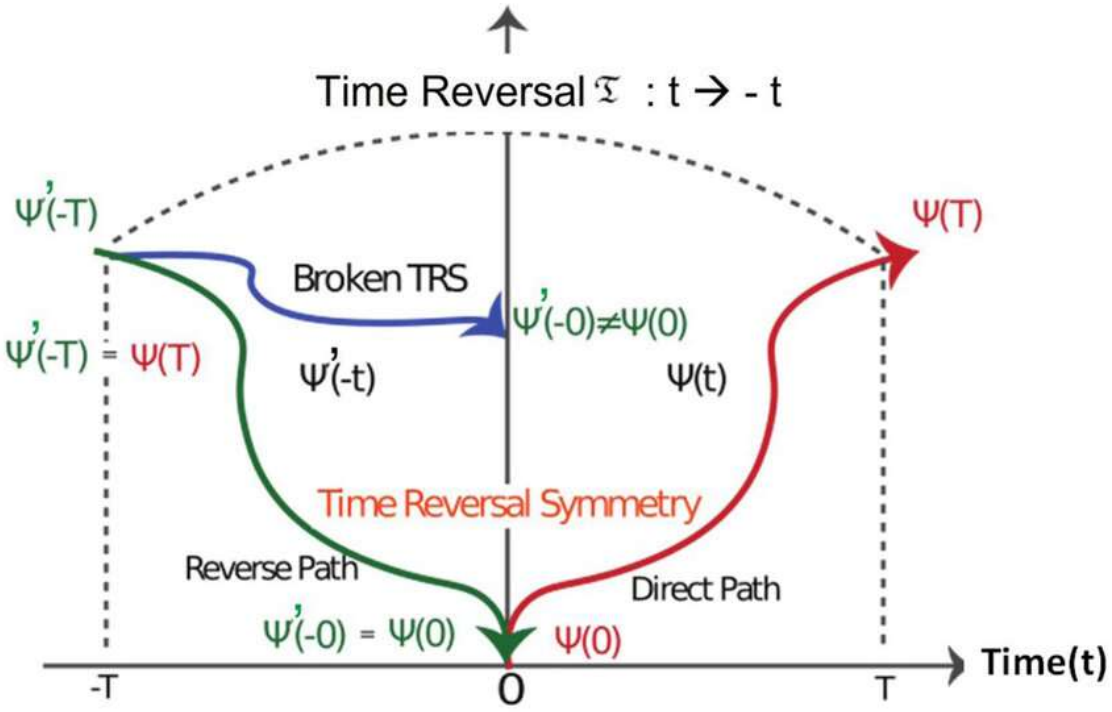
Time Reversal 𝒯 : t → - t
Ψ'(-T)
Ψ(T)
Broken TRS
Ψ'(-0)≠Ψ(0)
Ψ'(-T) = Ψ(T)
Ψ'(-t)
Ψ(t)
Time Reversal Symmetry
Reverse Path
Direct Path
Ψ'(-0) = Ψ(0)
Ψ(0)
Time(t)
-T
0
T

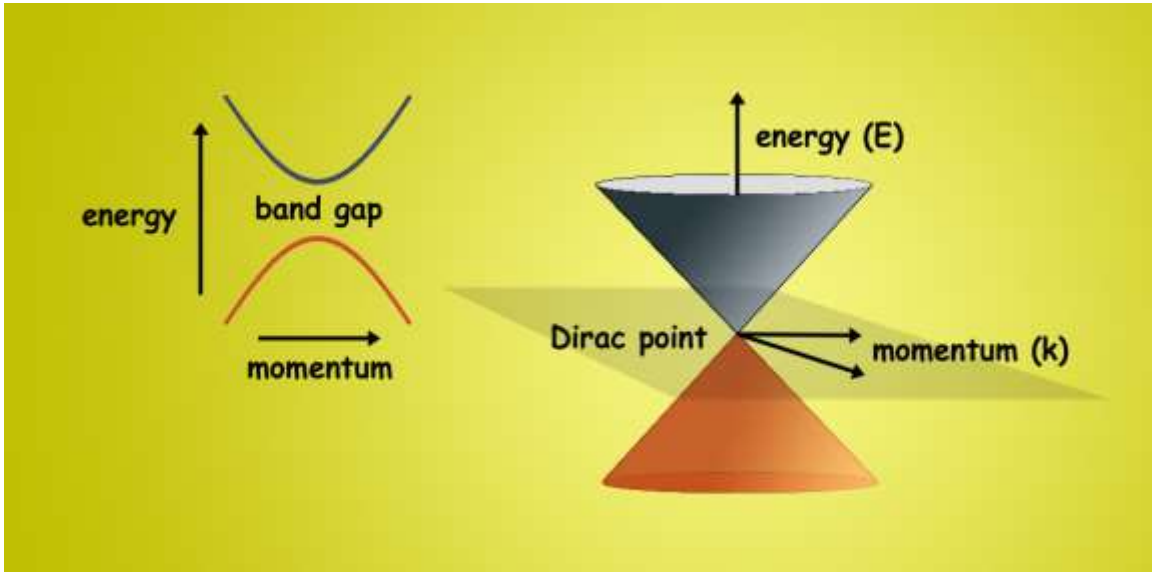
energy
band gap
momentum
energy (E)
Dirac point
momentum (k)

Time-reversal symmetry does exist in certain quantum materials, and it plays a crucial role in understanding the fundamental properties of these materials.

What is Time-Reversal Symmetry?

Time-reversal symmetry refers to the idea that the physical laws governing a system are invariant (or unchanged) when time is reversed.

In quantum mechanics, time-reversal symmetry involves the operation of reversing the momentum and spin of particles.

For example:

- $\vec{p} \rightarrow -\vec{p}$
- $\vec{S} \rightarrow -\vec{S}$

Time-Reversal Symmetry in Quantum Materials

Quantum materials often exhibit time-reversal symmetry, but the behavior of this symmetry depends on the type of material and the interactions present in the system. Here's how time-reversal symmetry can manifest or be broken in quantum materials:

1. Time-Reversal Symmetry in Topological Insulators

- Topological insulators are materials that have insulating bulk properties but conductive surface states that are protected by time-reversal symmetry. The surface states are robust against perturbations (like impurities or defects) because the time-reversal symmetry guarantees the protection of these edge states.
- In topological insulators, the spin of electrons is locked perpendicular to their momentum (this is called the **spin-momentum locking**), which is a result of time-reversal symmetry. If time-reversal symmetry is broken, these surface states can be destroyed, and the material's topological protection would be lost.

2. Time-Reversal Symmetry in Superconductors

•In conventional superconductors (which exhibit **BCS superconductivity**), time-reversal symmetry is generally preserved. The Cooper pairs (which are pairs of electrons that form the superconducting state) are in a state where time-reversal symmetry holds.

•However, in **topological superconductors**, the superconducting state may be sensitive to time-reversal symmetry breaking. In these materials, breaking time-reversal symmetry can lead to exotic phenomena, like the creation of **Majorana fermions**, which are potential candidates for quantum computing.

3. Magnetic Materials and Time-Reversal Symmetry

•**Magnetic materials** can either preserve or break time-reversal symmetry, depending on the type of magnetism they exhibit. For example, ferromagnetic materials typically break time-reversal symmetry because the magnetization is aligned in a particular direction and would change under time reversal.

•On the other hand, **antiferromagnetic materials**, where adjacent spins are aligned in opposite directions, can maintain time-reversal symmetry because reversing time would reverse the direction of all spins, but the overall symmetry is still preserved.

4. Quantum Hall Systems

•In the **quantum Hall effect**, time-reversal symmetry is typically broken in the presence of a magnetic field. The magnetic field forces the electrons to move in circular orbits, breaking the symmetry of the system.

•However, in the **quantum spin Hall effect** (which is a topological phenomenon), time-reversal symmetry is preserved, and the system exhibits robust edge states similar to those found in topological insulators.

Plan of the talk

- Why Topological Insulator?
- Basics of Topological Insulator
- Material preparation and characterizations
- Device Fabrication and Results
- Conclusions

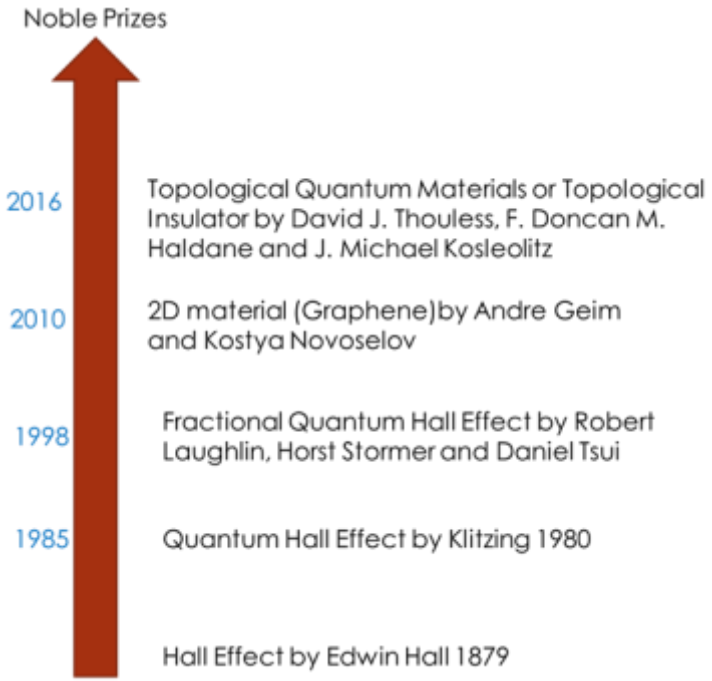

Size and restricted geometry => quantum confinement, enhanced many-electron interaction, reduced dimensionality, and symmetry effects

- Novel properties and phenomena
- Useful in applications, e.g., optoelectronics, energy conversion/generation, etc.
- Tunable properties by gating and environmental screening

Travel of electrons in a device

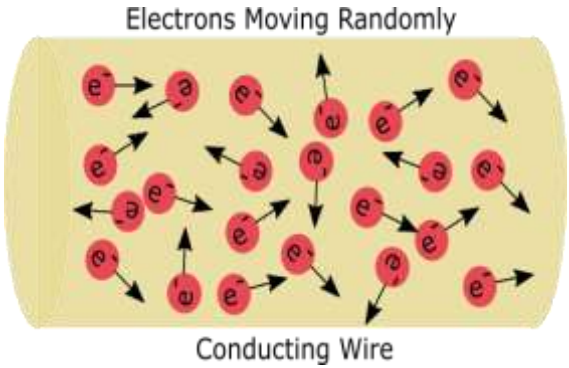

Tokura, Y., Yasuda, K., & Tsukazaki, A. (2019). Magnetic topological insulators. *Nature Reviews Physics*, *1*(2), 126-143.

Separate the electron motion

Hasan, M. Z., & Moore, J. E. (2011). Three-dimensional topological insulators. *Annu. Rev. Condens. Matter Phys.*, *2*(1), 55-78.

Baldomir, D., & Faílde, D. (2019). On behind the physics of the thermoelectricity of topological insulators. *Scientific reports*, *9*(1), 6324.

Condensed Matter Physics: Bands

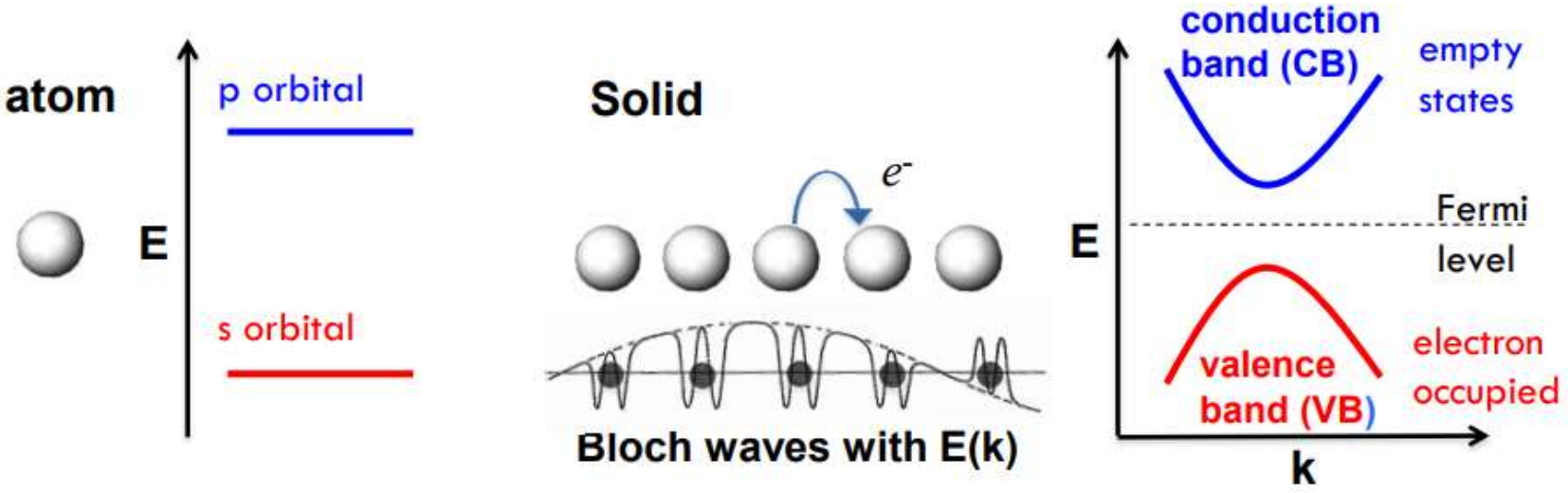

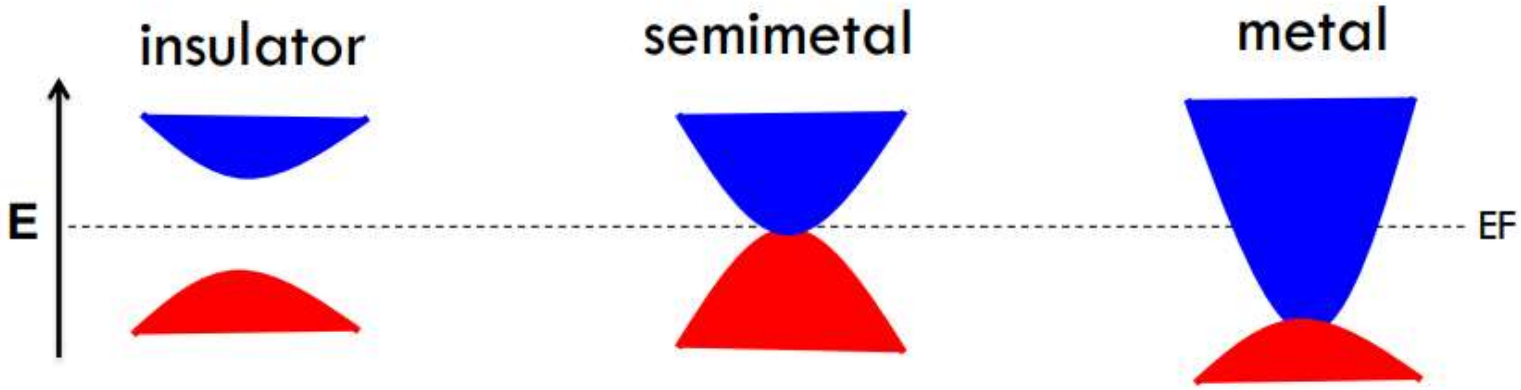

https://www.nanowerk.com/topological-insulators-explained.php
https://en.wikipedia.org/wiki/Topological_insulator

Metals and Insulators

Free electron

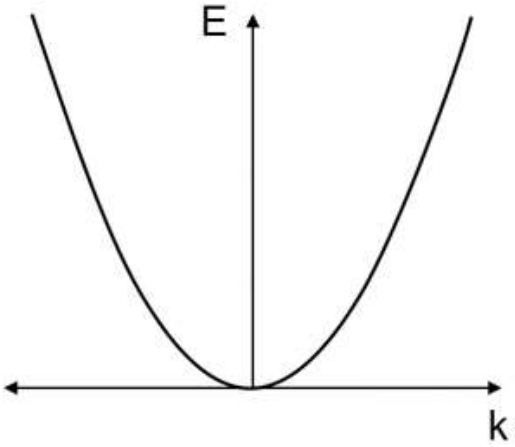

$$H = \frac{\hbar^2 k^2}{2m}$$

"Nearly free electron"

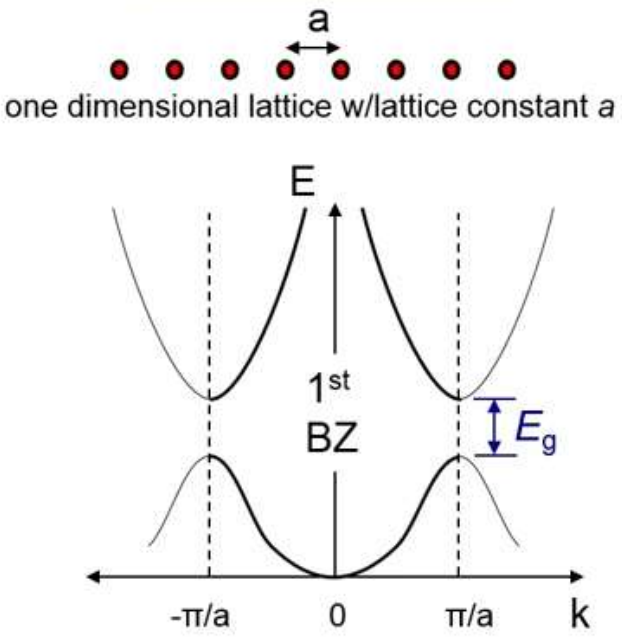

Metals and Insulators

"Nearly free electron"

one dimensional lattice w/lattice constant *a*

Two electrons (spin up, spin down) needed to fill a band

One electron per atom: Metal

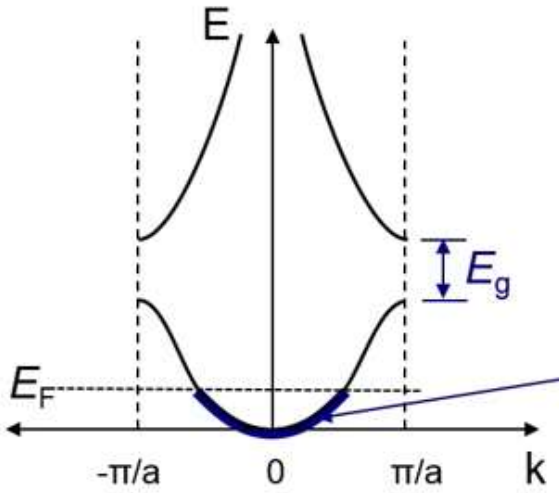

filled states

Two electrons per atom: Insulator

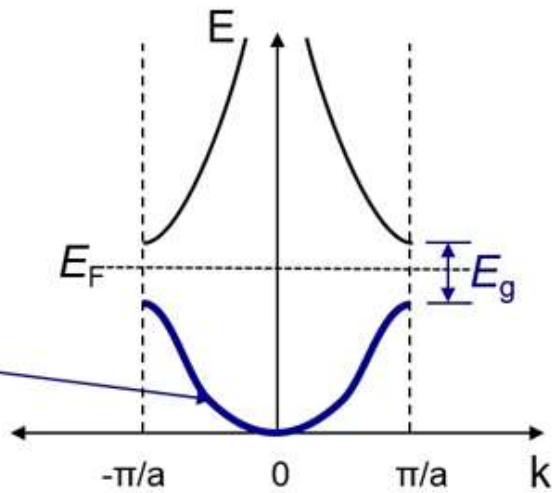

Metals and Insulators

"Nearly free electron"

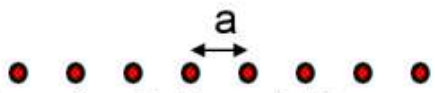

one dimensional lattice w/lattice constant *a*

Two electrons (spin up, spin down) needed to fill a band

One electron per atom: Metal

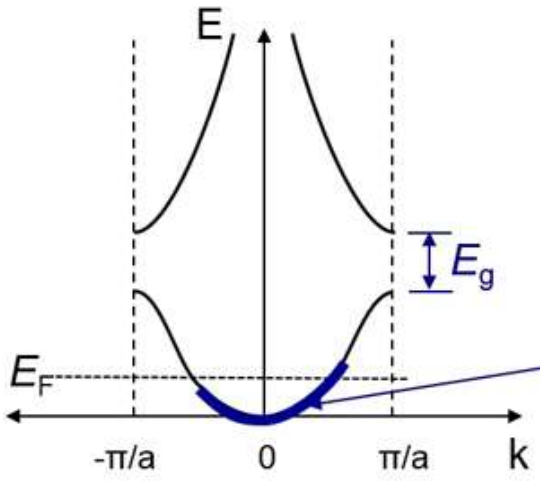

filled states

Two electrons per atom: Insulator

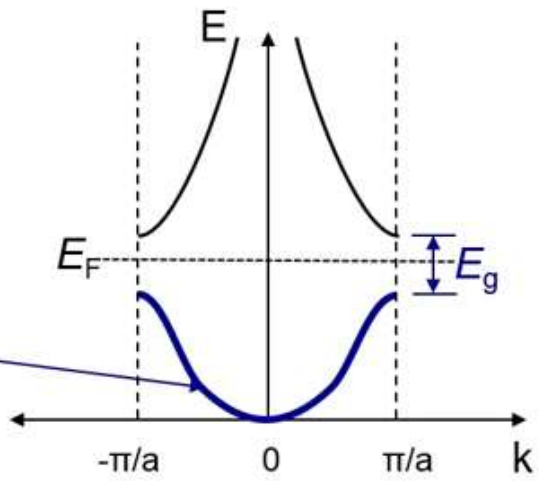

Electric Field

+k states populated over –k states
Current flows

Electric Field

No change in occupied states
No current flows

Hall Effect

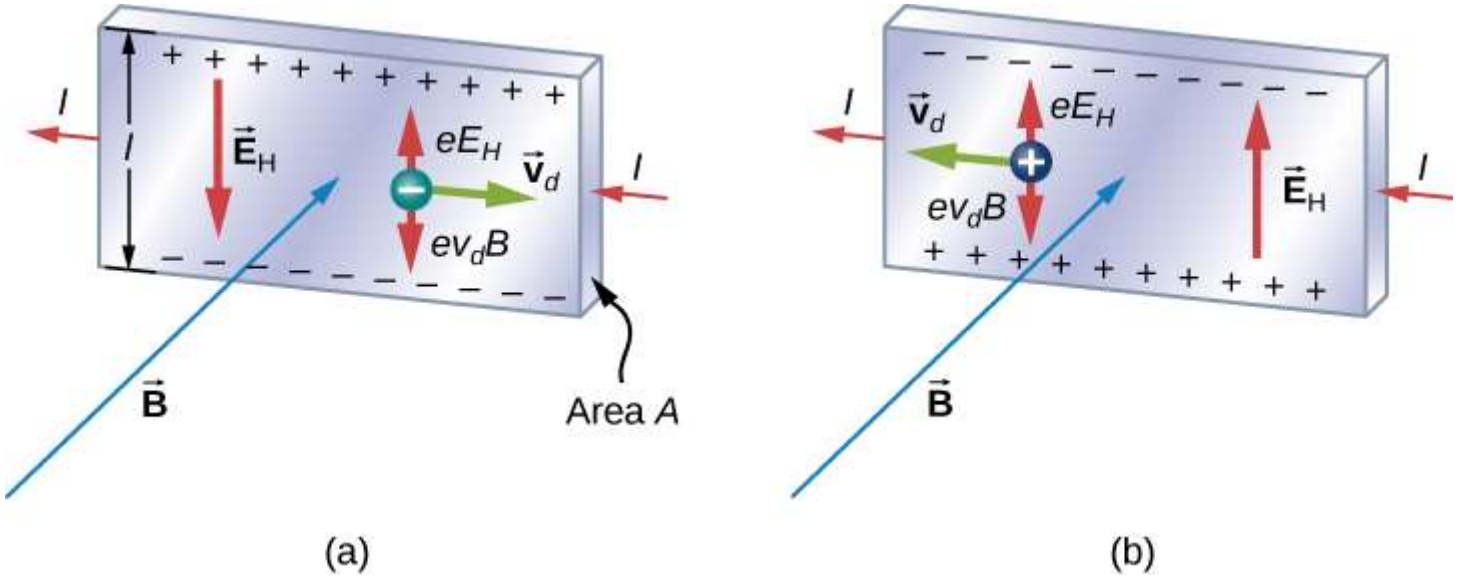

In the Hall effect, a potential difference between the top and bottom edges of the metal strip is produced when moving charge carriers are deflected by the magnetic field. (a) Hall effect for negative charge carriers; (b) Hall effect for positive charge carriers.

- In Equilibrium condition
- $$eE_H = ev_d B_z$$

$$v_d = \frac{E_H}{B_z}$$

- Sigh of predominant charge
- Charge density (n)
- Mobility

$$J = \sigma \mathbf{E} = en\mu_n \mathbf{E}$$

- Drift speed

$$I_x = -nev_d A$$

- Current

$$I_x = -ne\left(\frac{E_H}{B_z}\right)A \qquad J_x = ne\left(\frac{E_H}{B_z}\right)$$

- As we know that

$$E_H = \frac{V_H}{l}$$

$$V_H = -\frac{IBl}{neA} \qquad V_H = -\frac{IBl}{netl} \qquad V_H = -\frac{IB}{net} \qquad R_H = -\frac{1}{ne}$$

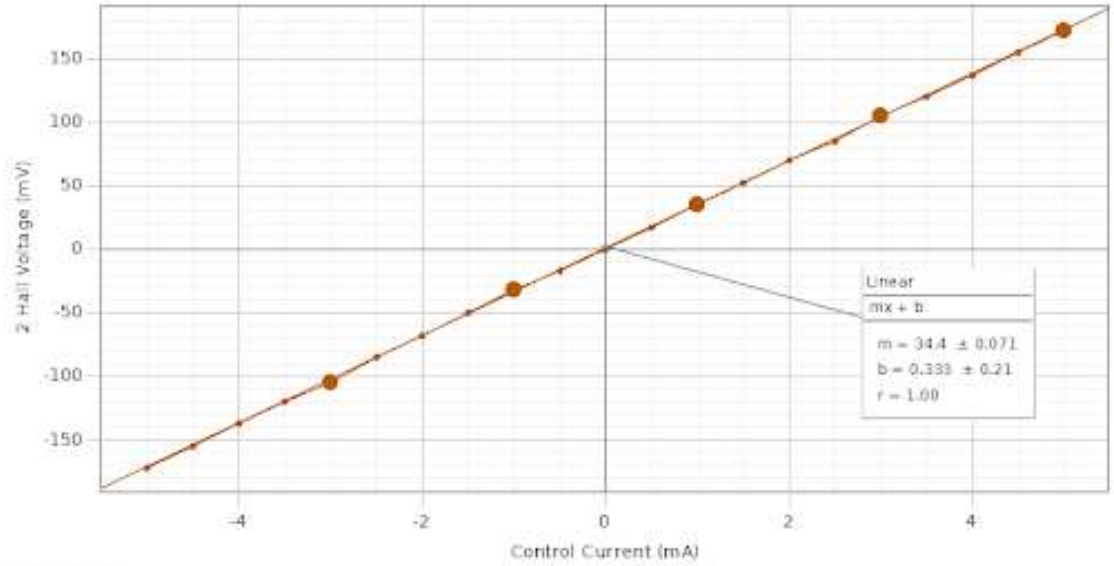
2 Hall Voltage (mV)
150
100
50
0
-50
-100
-150
-4
-2
0
2
4
Control Current (mA)
Linear
mx + b
m = 34.4 ± 0.071
b = 0.333 ± 0.21
r = 1.00

[B=200mT]

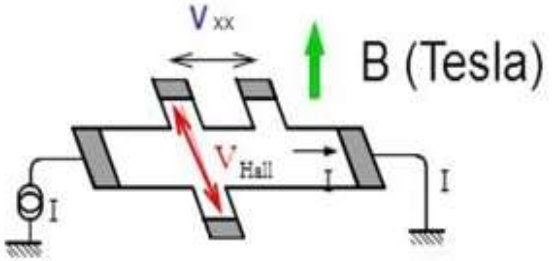
V xx
B (Tesla)
V Hall
I
I

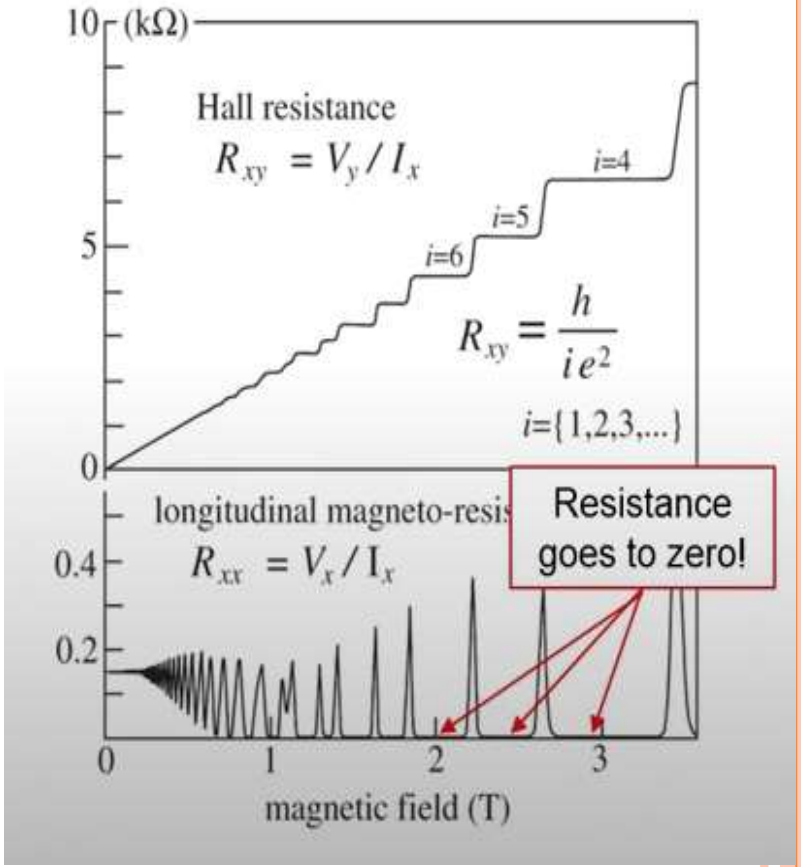
10
(kΩ)
Hall resistance
$R_{xy} = V_y / I_x$
i=4
i=5
i=6
5
$R_{xy} = \frac{h}{ie^2}$
i={1,2,3,...}
0
longitudinal magneto-resis
$R_{xx} = V_x / I_x$
Resistance goes to zero!
0.4
0.2
0
1
2
3
magnetic field (T)

Importance of the dimensionality

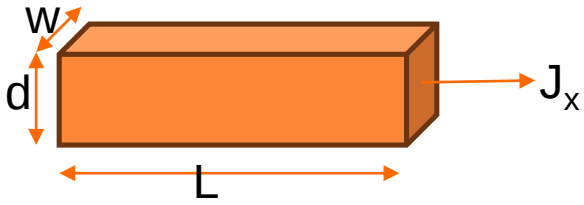

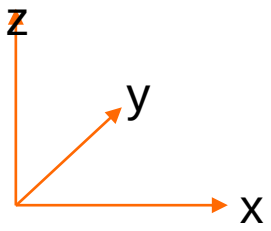

In 3d, current flow in x-direction so $J_y=0$

$$\begin{pmatrix} \frac{E_x}{E_y} \end{pmatrix} = \begin{pmatrix} \rho_{xx} & \rho_{xy} \\ -\rho_{xy} & \rho_{xx} \end{pmatrix} \begin{pmatrix} \frac{J_x}{0} \end{pmatrix}$$

$$\begin{pmatrix} \frac{E_x}{E_y} \end{pmatrix} = \begin{pmatrix} \frac{\rho_{xx} J_x}{-\rho_{xy} J_x} \end{pmatrix}$$

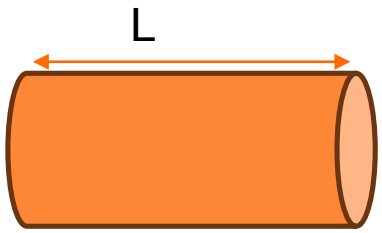

$R=\rho L/A$
If $A=L^2$
$R=\rho L/ L^2$
$R=\rho/L$

$R=\rho L^{2-D}$

Resistivity

$$\rho_{xx} = \frac{E_x}{J_x} \qquad R_{xx} = \frac{V_x}{I_x} = \frac{E_x L}{J_x A} = \rho_{xx}\left(\frac{L}{A}\right)$$

$$\rho_{xy} = \frac{-E_y}{J_x} \qquad R_{xy} = -\frac{V_y}{I_x} = -\frac{E_y w}{J_x A} = \rho_{xy}\left(\frac{w}{A}\right)$$

D=3 $R=\rho/L$
D=2 $R=\rho$

$$R_{xx} = \frac{V_x}{I_x} = \frac{E_x L}{J_x w} = \rho_{xx}\left(\frac{L}{w}\right)$$

$$R_{xy} = -\frac{V_y}{I_x} = -\frac{E_y w}{J_x w} = \rho_{xy}$$

Density of States

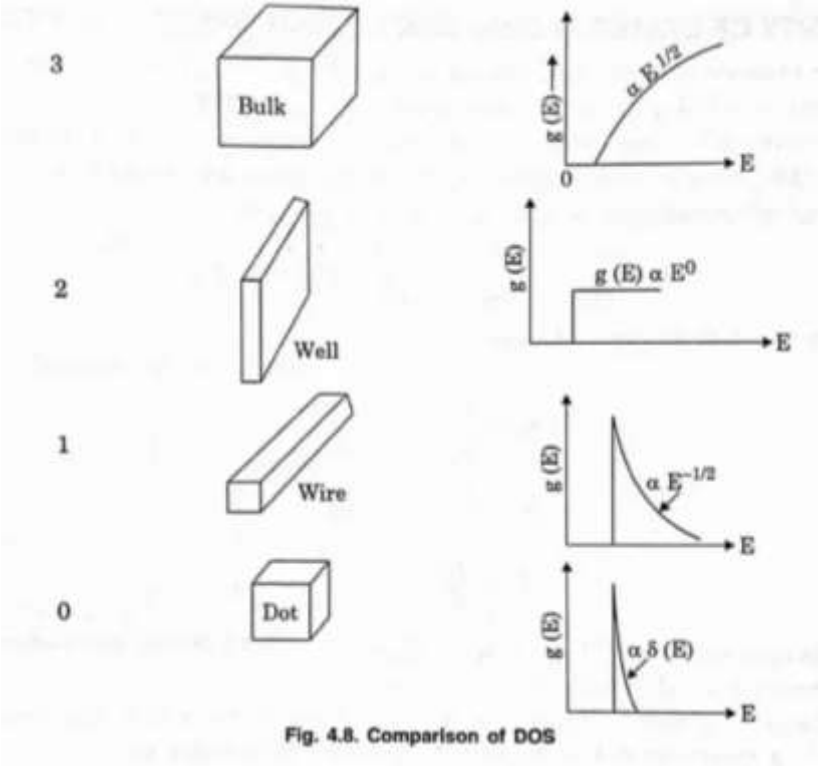

Fig. 4.8. Comparison of DOS

Quantum Mechanics of a Charge in Magnetic filed

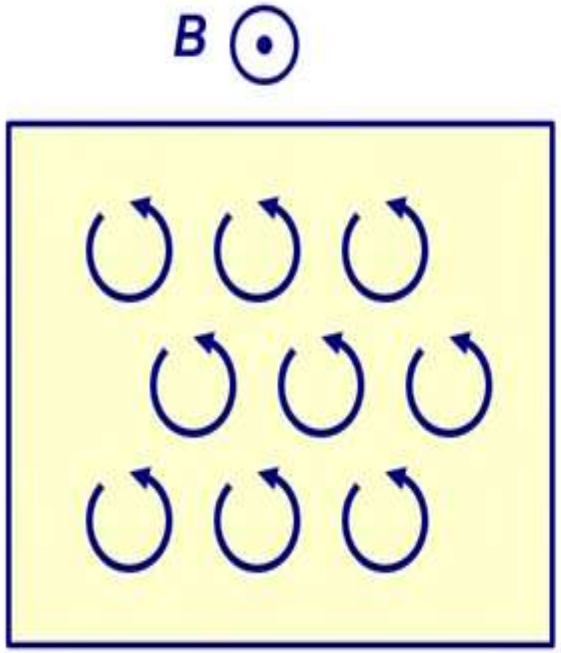

$$-\frac{\hbar^2}{2m}\nabla^2\psi(\vec{r})+ V(\vec{r})\psi(\vec{r}) = E\ \psi(\vec{r})$$

$$V(\vec{r})=0$$

$$-\frac{\hbar^2}{2m}\nabla^2\psi(\vec{r})=E\ \psi(\vec{r})$$

$$\frac{p^2}{2m}\psi(\vec{r})= E\psi(\vec{r})$$

$$\vec{p} \rightarrow \vec{p} - q\vec{A}$$

$$B = \vec{\nabla} \times \vec{A}$$

B in z-direction

A may be in x or y direction

$$\vec{A} = (-By, 0, 0)$$

$$\vec{A} = (0, Bx, 0)$$

$$\vec{A} = (\frac{By}{2}, -Bx/2, 0)$$

$$[\frac{(p_x - eBy)^2}{2m} + \frac{p_y^2}{2m} + \frac{p_z^2}{2m}]\psi(\vec{r})= E\psi(\vec{r})$$

The motion in z-direction is like free particle and its quantized in z-direction

$$[\frac{(p_x - eBy)^2}{2m} + \frac{p_y^2}{2m}]\psi(\vec{r})= E\psi(\vec{r})$$

$[p_x, H(x,y)] = 0$ conserved $p_x = \hbar k$

$[p_y, H(x,y)] = i\hbar$

Quantum Mechanics of a Charge in Magnetic filed

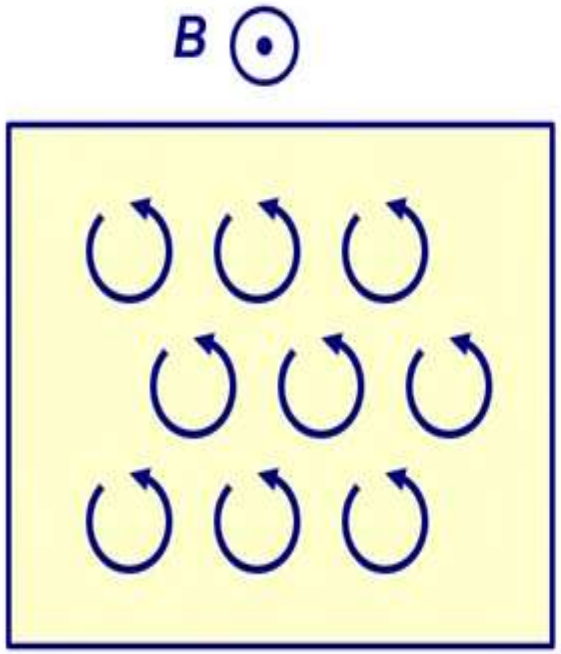

$$[p_y, H(x,y)] = i\hbar$$

$$[\frac{(p_x - eBy)^2}{2m} + \frac{p_y^2}{2m}]\psi(\vec{r}) = E\psi(\vec{r})$$

$$[\frac{(\hbar k - eBy)^2}{2m} + \frac{p_y^2}{2m}]\psi(\vec{r}) = E\psi(\vec{r})$$

$$[\frac{p_y^2}{2m} + \frac{1}{2}m\left(\frac{eB}{m}\right)(\frac{\hbar k}{eB} - y)^2 \ ]\psi(\vec{r}) = E\psi(\vec{r})$$

$$[\frac{p_y^2}{2m} + \frac{1}{2}m\left(\frac{eB}{m}\right)(y - \frac{\hbar k}{eB})^2 \ ]\psi(\vec{r}) = E\psi(\vec{r})$$

$$[\frac{p_y^2}{2m} + \frac{1}{2}m\left(\frac{eB}{m}\right)(y - l_B)^2 \ ]\psi(\vec{r}) = E\psi(\vec{r})$$

H.O osscillation along $y-$ direction about magnetic lengh $l_B = \frac{\hbar k}{eB}$

- Localized in space, $v_{group} = 0$
- Highly degenerate with discrete energies:

$$E = \left(n + \frac{1}{2}\right)\hbar\omega_c \qquad \omega_c = \frac{eB}{m}$$

- "Landau levels"

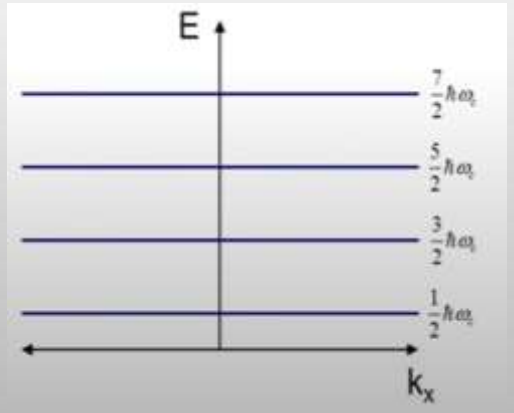

Is 2D electron system with filled Landau levels an insulator?

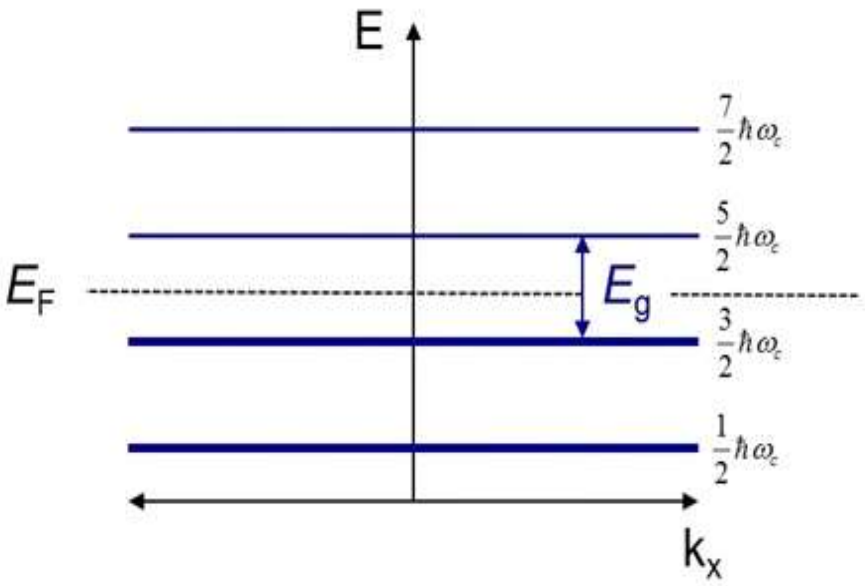

Experiment: clean 2D semiconductor

($\omega_c\tau = \mu B >> 1$)

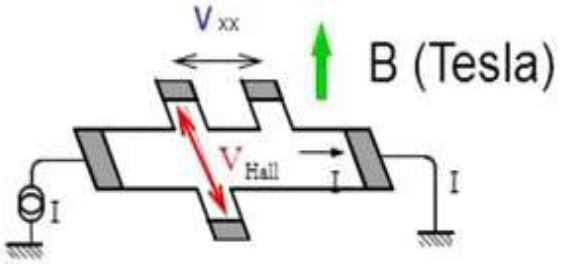

Degeneracy of Landau levels

$$y_0 = l_B = \frac{p_x}{eB} = \frac{\hbar k_x}{eB} = \frac{\hbar 2\pi n_x}{eBL_x}$$

Maximum degeneracy of Landau levels

$$g = (n_x)_{max} = \frac{eBL_xL_y}{2\pi\hbar} = \frac{eBA}{2\pi\hbar} = \frac{BA}{h/e} = \frac{BA}{\phi_0}$$

ϕ_0=h/e flux quanta

Degeneracy can be infinite

Landau Levels are flat

Velocity of Electron $V_k = \frac{1}{\hbar}\frac{\partial E}{\partial k} = 0$ ⇒ K.E.=0 So, only energy remain is only P.E.

Is 2D electron system with filled Landau levels an insulator?

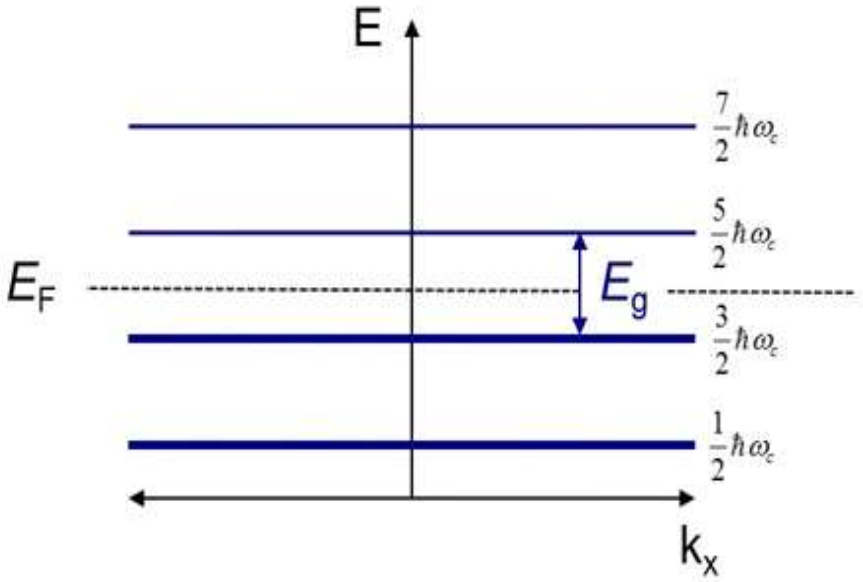

Experiment: clean 2D semiconductor

($\omega_c\tau = \mu B >> 1$)

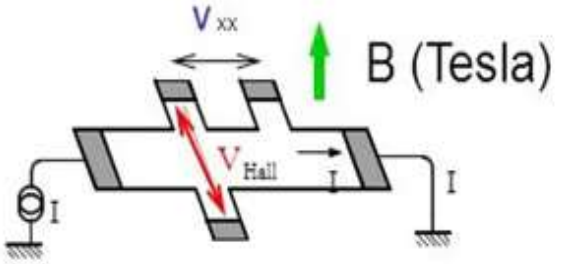

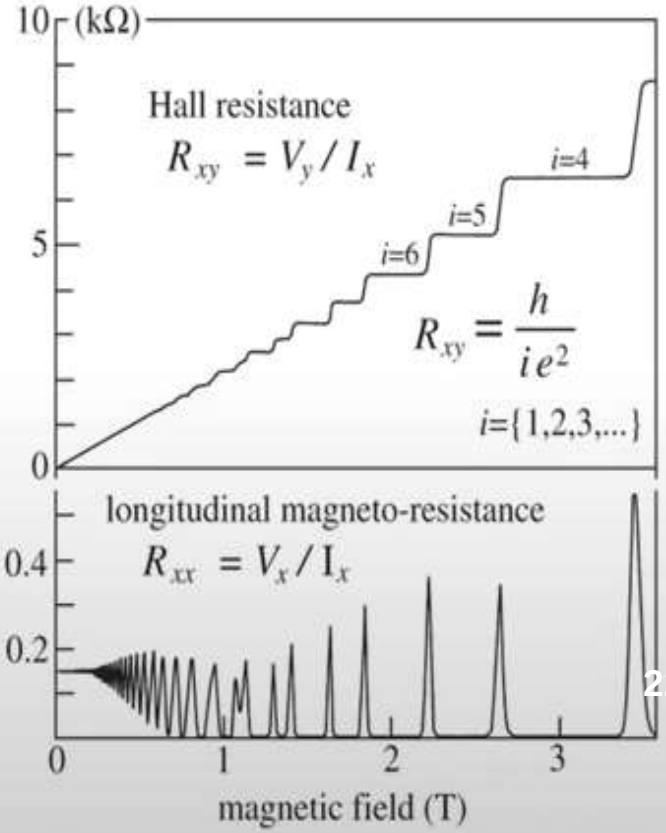

$$\rho_{xy}=R_{xy}=\rho_H=\frac{h}{ie^2}$$

i is related to degeneracy with following way

$$i=\frac{n_0}{g/A}=\frac{n_0}{eB/h}=\frac{n_0}{\frac{B}{h/e}}=\frac{n_0\phi_0}{B}$$

ϕ_0=h/e= 4.13x10^{-15} wb

$$i=\frac{n_0}{g}=\frac{n_0}{eAB/h}=\frac{n_0}{\frac{AB}{h/e}}=\frac{n_0\phi_0}{AB}=\frac{n_0}{\varphi/\phi_0}$$

Is 2D electron system with filled Landau levels an insulator?

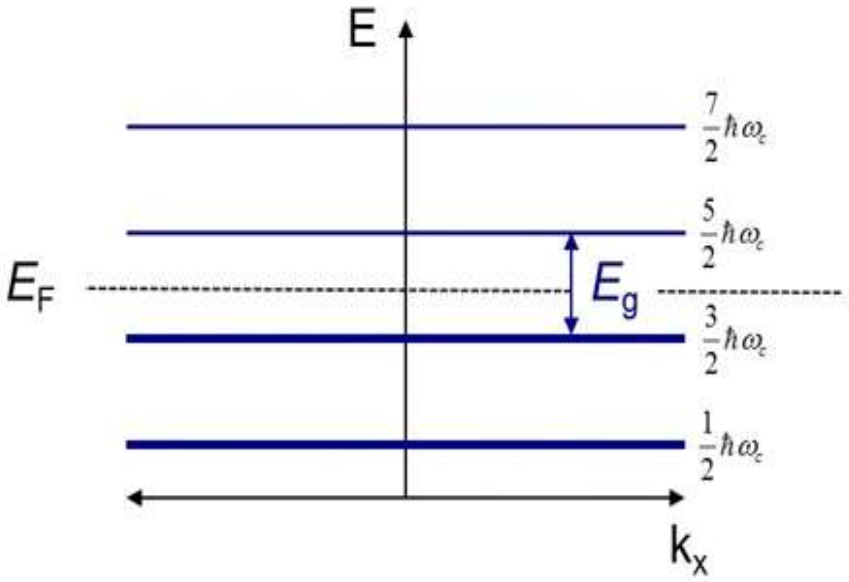

$$\psi(x,y) = e^{ik_x x} f(y) = \frac{1}{\sqrt{L_x}} e^{ik_x x} \; A_n e^{\frac{eB(y-y_0)^2}{\hbar}} H_n\left(\frac{eB(y-y_0)}{\hbar}\right)$$

Conductivity of Landau Levels $V_k = \frac{1}{\hbar}\frac{\partial E}{\partial k}$=0

$$\langle J_x \rangle = -\frac{e}{m}\langle \psi(x,y)|(p+eA)|\psi(x,y)\rangle = 0$$

Experiment: clean 2D semiconductor

($\omega_c\tau = \mu B >> 1$)

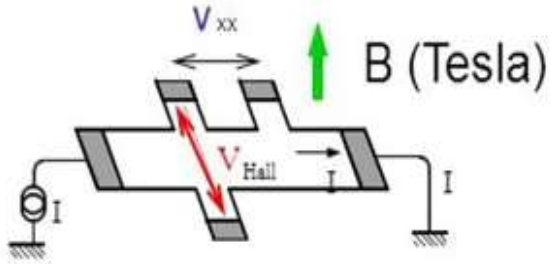

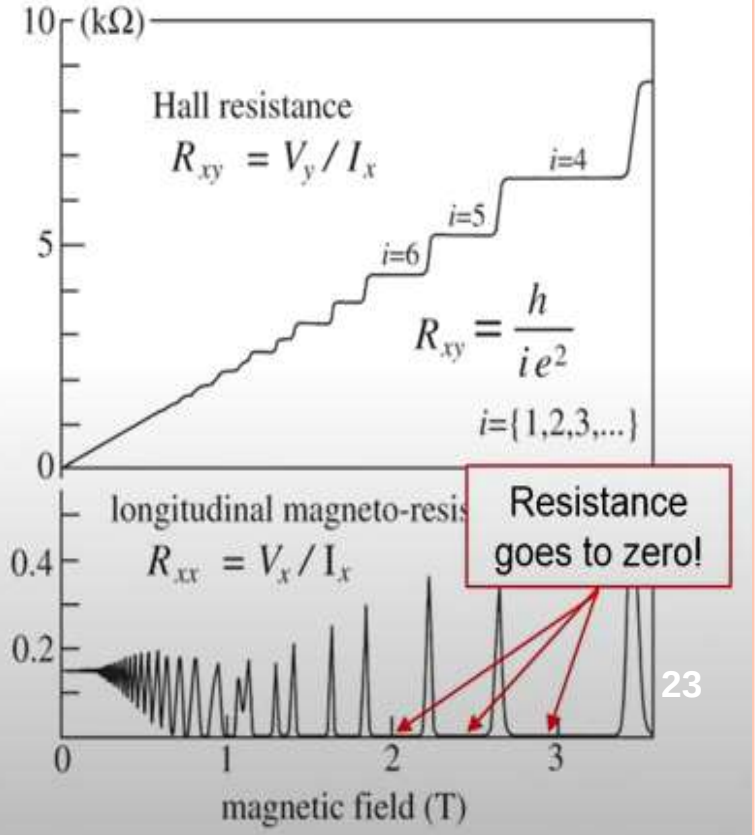

Different view: the edge state picture of quantum Hall

$$H = \frac{1}{2m}\left[{p_x}^2 + \left(p_y - eBx\right)^2\right] + eEx$$

$$\epsilon_{n,k} = (n + 1/2)\hbar\omega_B - eE\left(kl_B^2 + \frac{eE}{m\omega_B^2}\right) + \frac{1}{2}m\frac{E^2}{B^2}$$

- Confining potential pushes up Landau levels at edges of sample
- Fermi energy crosses Landau levels
- → 1D edge states carry current in **E** x **B** direction

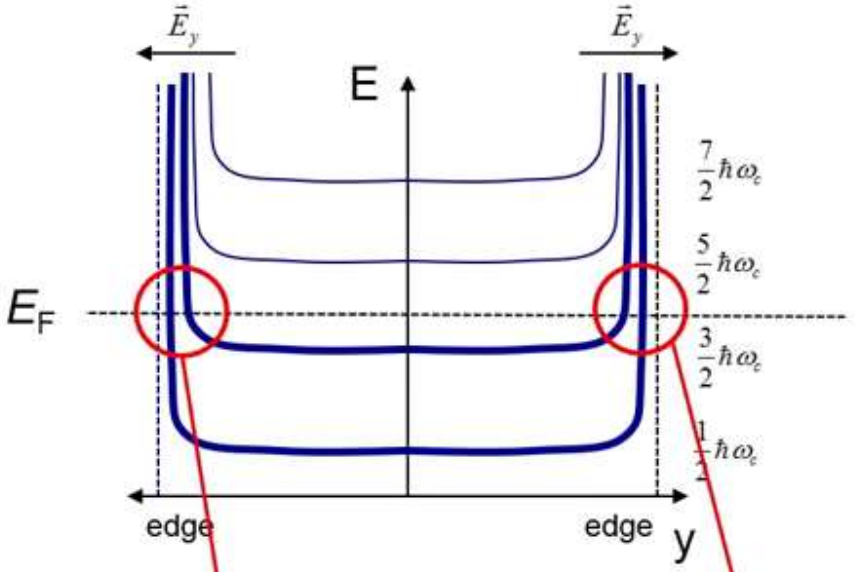

$$V_y = -\frac{1}{\hbar}\frac{\partial\epsilon_{n,k}}{\partial k} = \text{E/B}$$

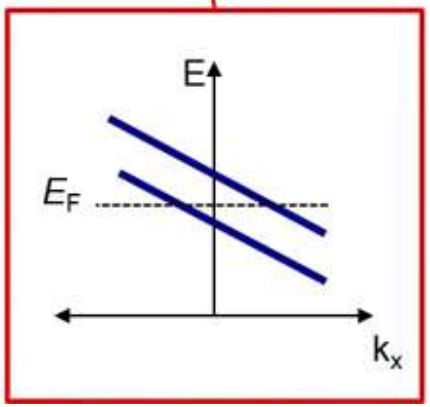

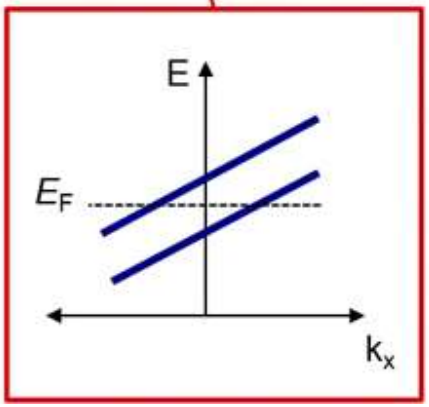

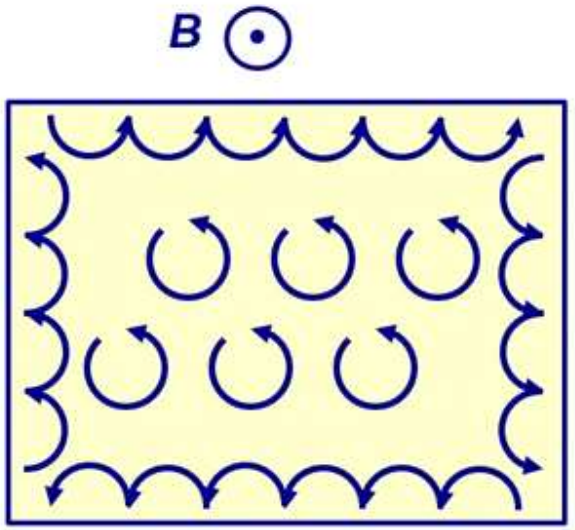

Classification of States of Matter

Spontaneous symmetry breaking, establishing an order parameter

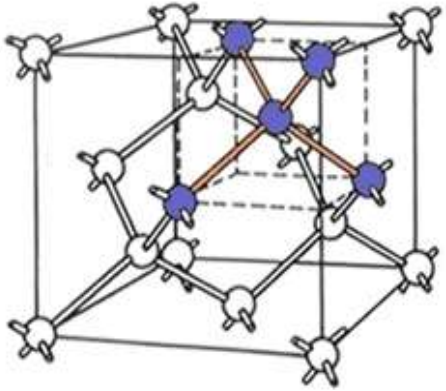

Crystal: Broken translational symmetry

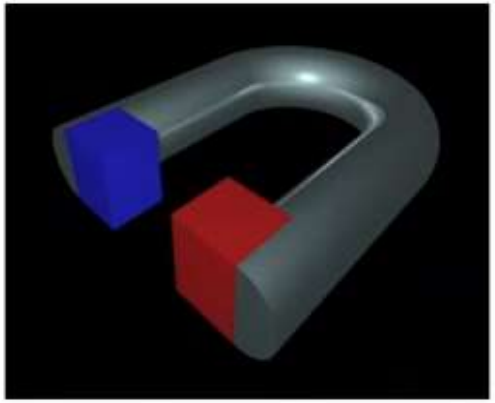

Magnet: Broken rotational symmetry

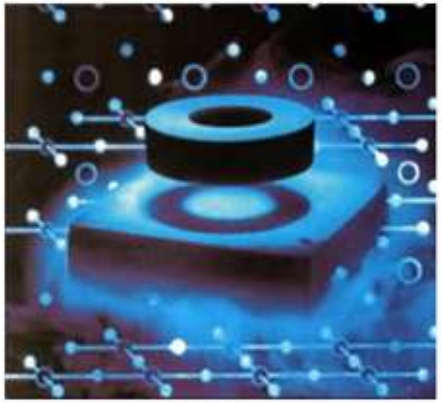

BCS Superconductor: Broken gauge symmetry

Reviews of topology and quantum phases:

Moore, *Nature 464*,194 (2010)

Hasan & Kane *Rev. Mod. Phys.* **82**, 3045 (2010)

Avron, Osadchy & Seiler, *Physics Today,* August 2003 p.38

Topology

topologically different from

$$\frac{1}{2\pi}\oint_{\substack{\text{closed}\\\text{surface}}} K dA = 2 - 2g$$

Gauss-Bonnet theorem

K is Gaussian curvature

g is genus of surface

$g = 0$

$g = 1$

Topology in Condensed Matter Physics

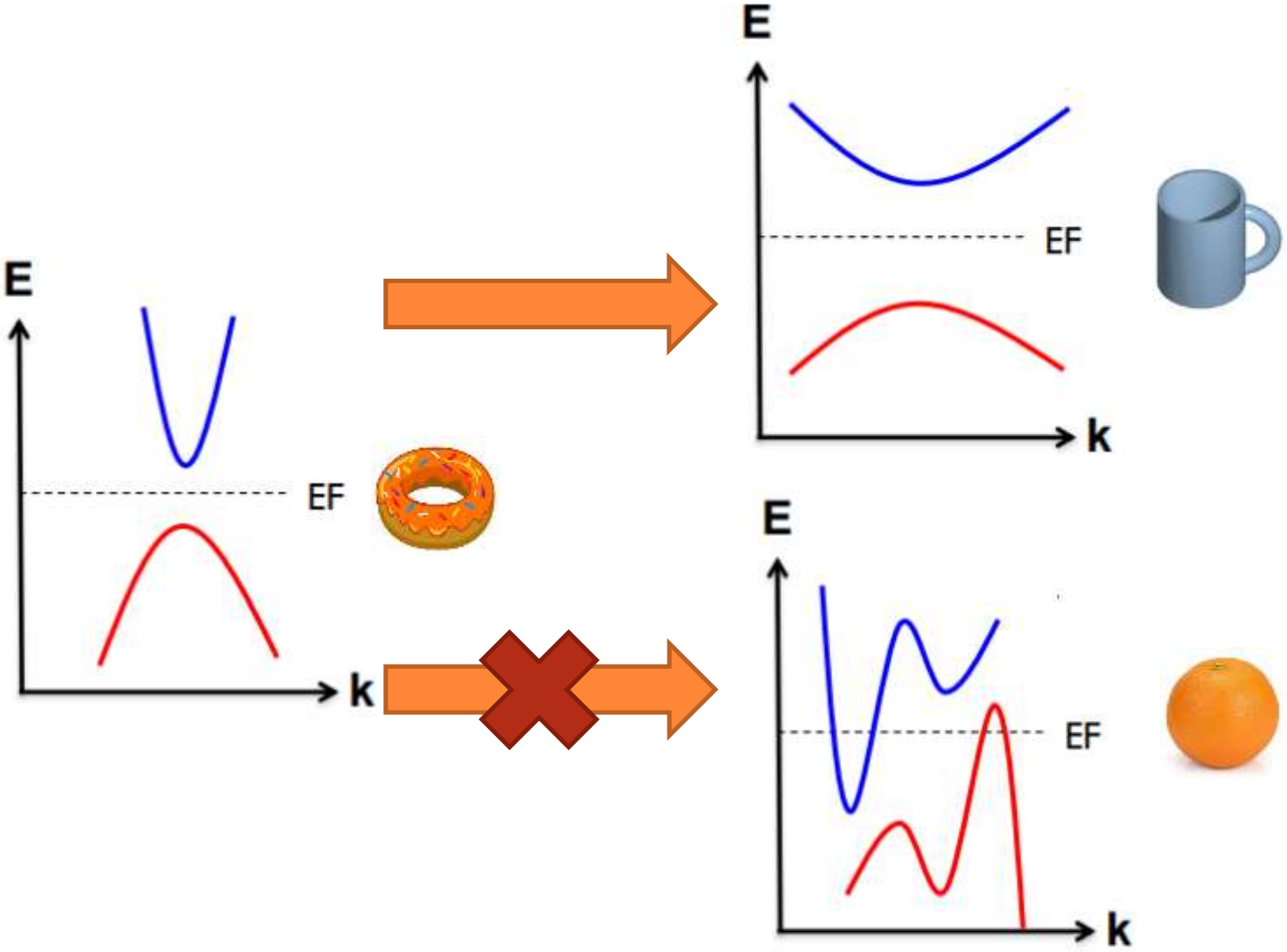

Colloquium: Topological insulators: https://doi.org/10.1103/RevModPhys.82.3045

Topology in Condensed Matter Physics

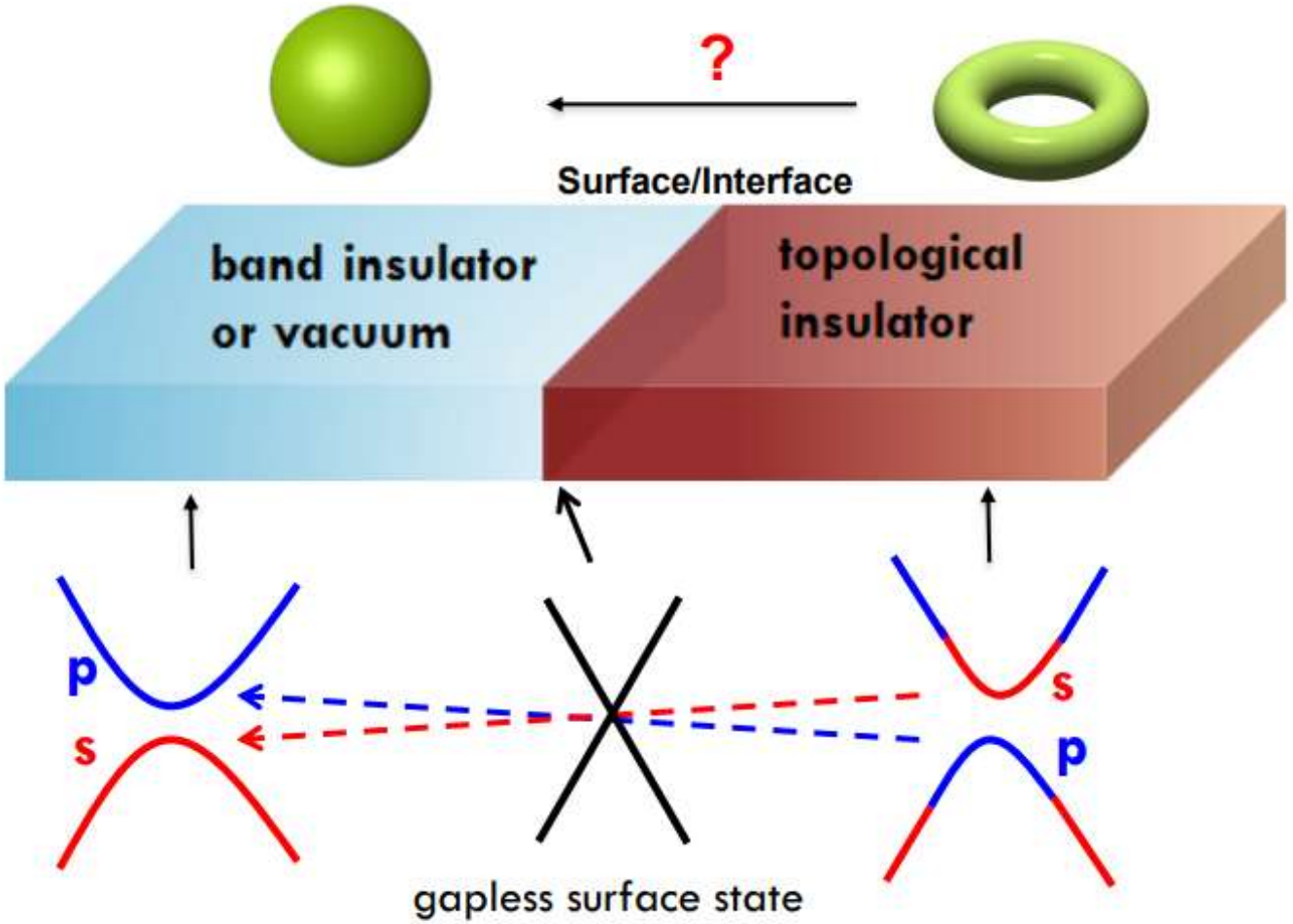

The gapless surface state is the hallmark of topological phase.

Topological Phases in Condensed Matter Physics by Saurabh Basu
https://ocw.tudelft.nl/courses/topology-condensed-matter-concept/
https://cmt-qo.phys.ethz.ch/education/spring-semester-2021.html

$h/ve^2 = 25.8\ k\Omega$

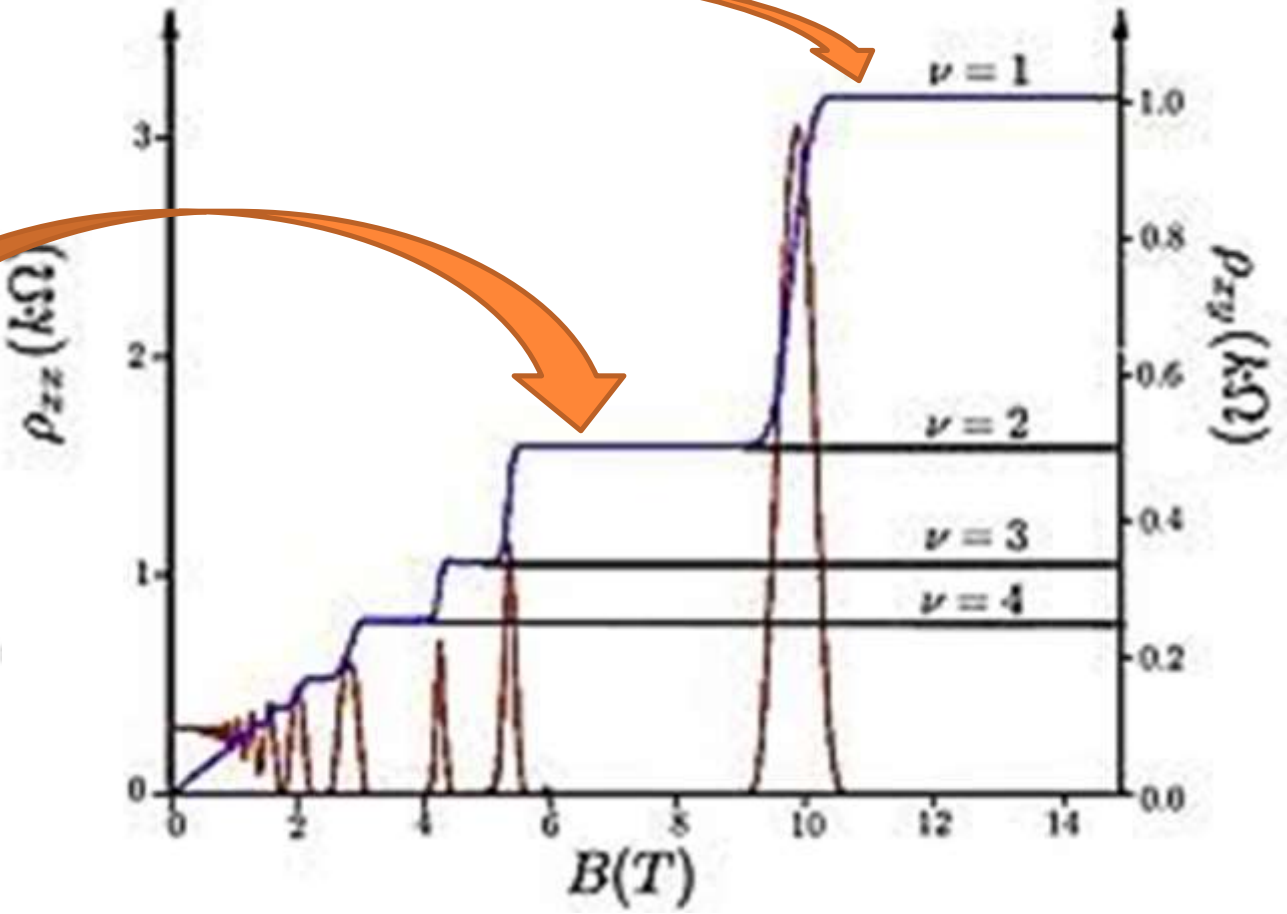

(a)

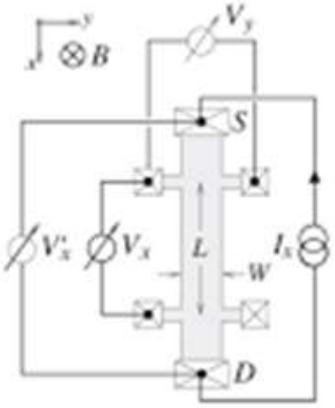

Planar Hall effect from the surface of topological insulators. .A.K Taskin et. el. https://doi.org/10.1038/s41467-017-01474-8

Topological Insulators

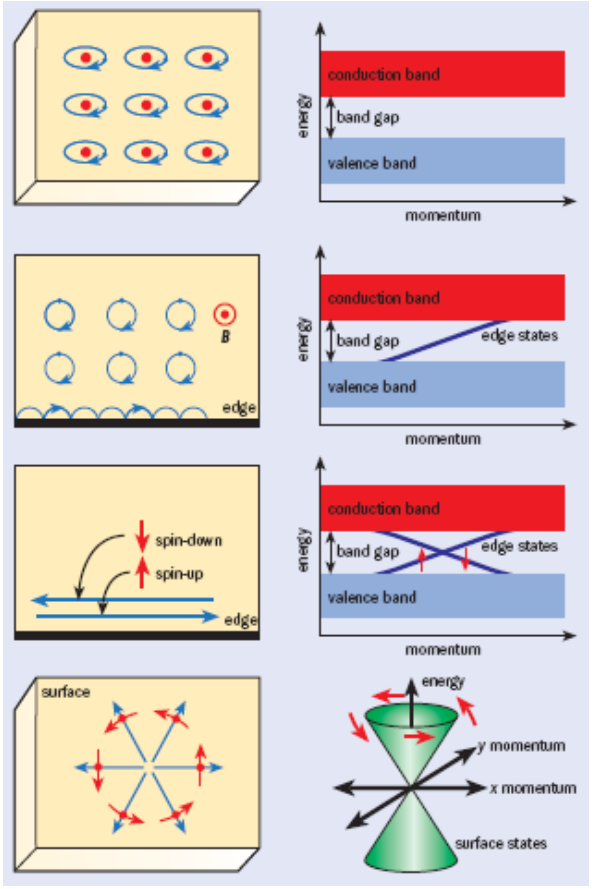

Insulator

Quantum Hall system

Kane et al. Science , 314, 1692 (2006)

Quantum spin Hall state:
2D topological insulator

3D topological insulator
2D surface shows Dirac cone with locking between spin and momentum

3D topological insulators: $Bi_X Sb_{1-x}$, Bi_2Se_3, Bi_2Te_3

Topological Insulators

Bi_2Te_3

Desalegne et al. Nano Lett. , 10, 1209 (2010)

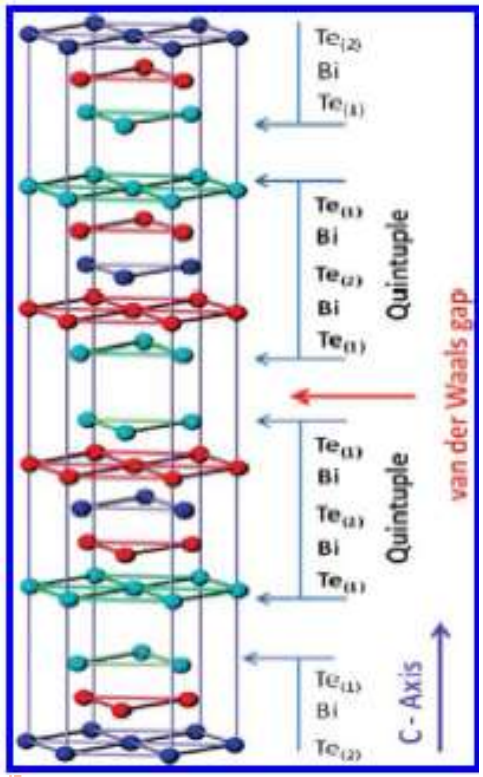

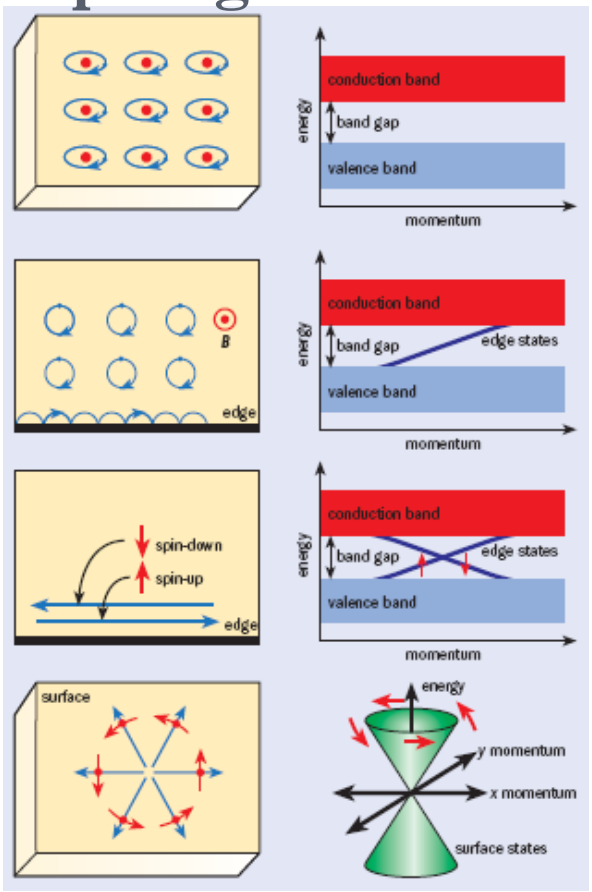

Insulator

Quantum Hall system

Quantum spin Hall state:
2D topological insulator

3D topological insulator
2D surface shows Dirac cone with locking between spin and momentum

3D topological insulators: $Bi_X Sb_{1-x}$, Bi_2Se_3, Bi_2Te_3

Topological Insulators

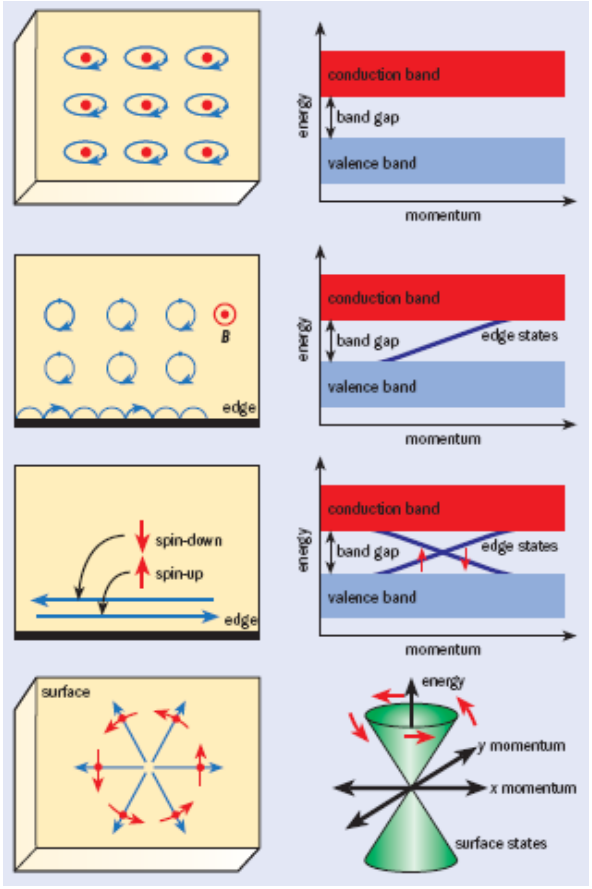

Insulator

Quantum Hall system

Kane et al. Science , 314, 1692 (2006)

Quantum spin Hall state:
2D topological insulator

3D topological insulator
2D surface shows Dirac cone with locking between spin and momentum

3D topological insulators: $Bi_X Sb_{1-x}$, Bi_2Se_3, Bi_2Te_3

Majorana fermion: a half integral spin particle that is its own antiparticle

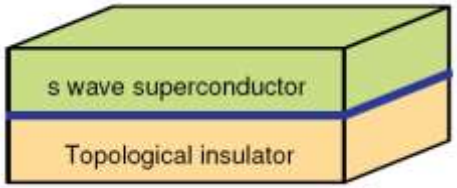

Proximity superconductivity on surface of 3D topological insulator → Majorana fermions

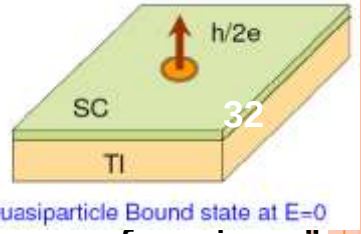

The goal: “Topological quantum computing with Majorana fermions”

Aim of our study: Examine 3D Topological insulator with superconducting contact

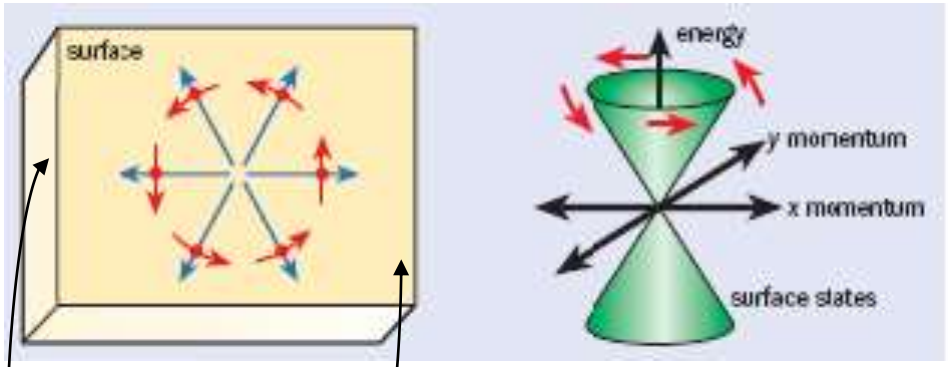

In: Superconductor

Proximity effect

2D Surface: Dirac cone

3D TI: Bi_2Te_3

Topological to Superconducting junctions

Experimental details

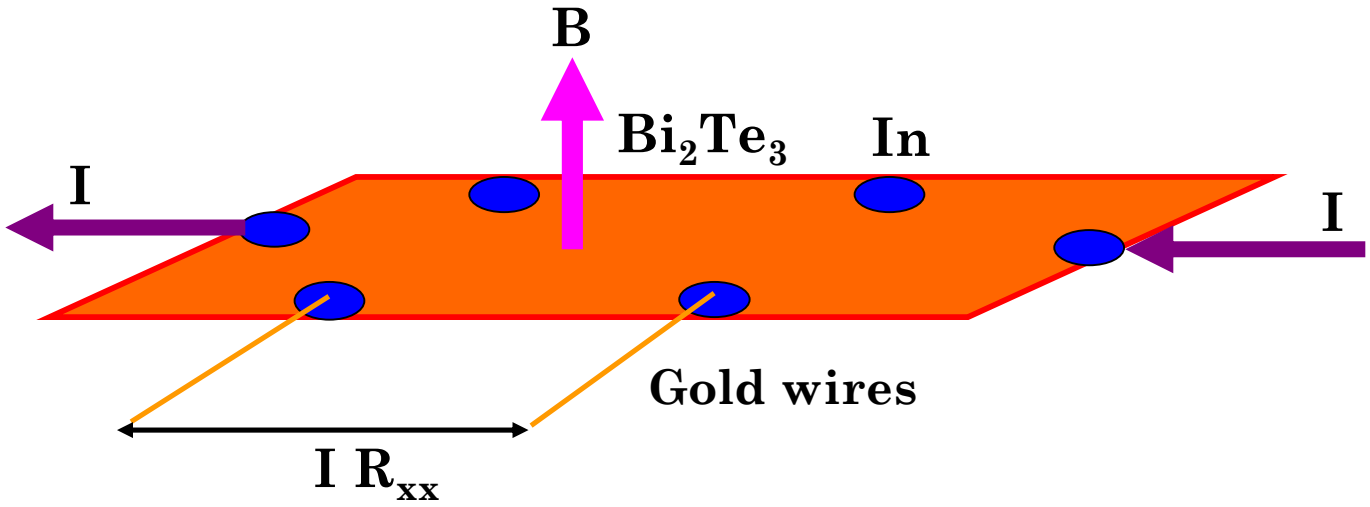

- Bi_2Te_3 samples prepared by mechanical exfoliation
- Contact on samples with Ag; In or Pb: (superconductors)
  - In: T_C = 3.4 K, Pb: T_C = 7.2 K
  - Ag is not a superconductor
- R_{xx} in temperature range of 1.5 to 10 K
- Magnetic field (B) orientation parallel to the axis C
- Standard lock-in technique
- Mobility ~ 1000-1200 $cm^2 V^{-1}S^{-1}$
- Carrier concentration ~ $1.9x10^{19}$ cm^{-3}

Results and Discussions

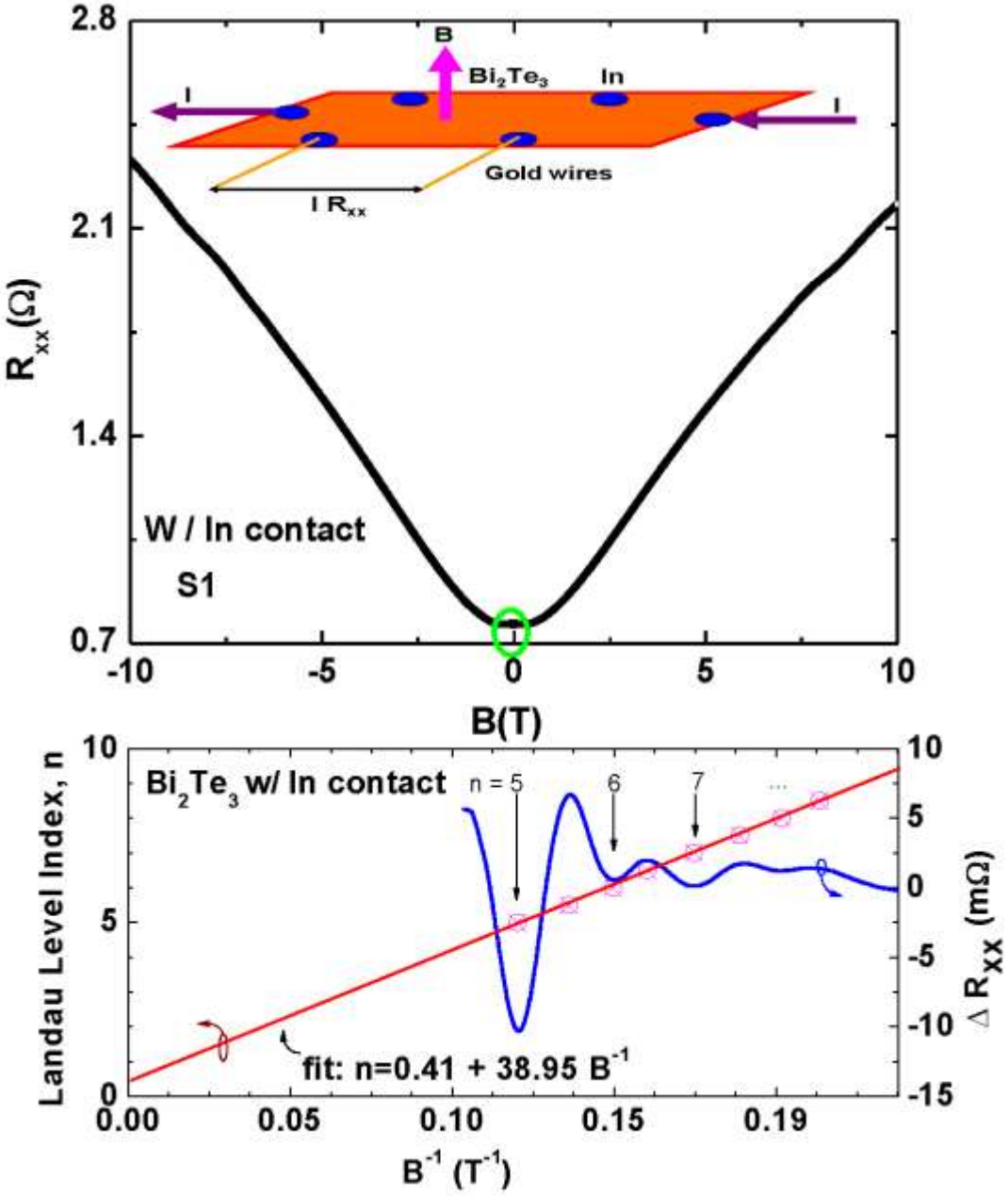

Longitudinal resistance (R_{xx}) of Bi_2Te_3 at 1.5 K in field range of ±10T. Inset shows the In contacts on the surface of Bi_2Te_3 flakes. Magnetic field applied along the C-axis and current is flowing within the plane .

Shubnikov-de Hass (SdH) oscillations (after subtracting 2nd order polynomial from R_{xx}) and Landau levels with inverse of magnetic fields and red line linear fitted data.

Negative resistance correction in Bi_2Te_3

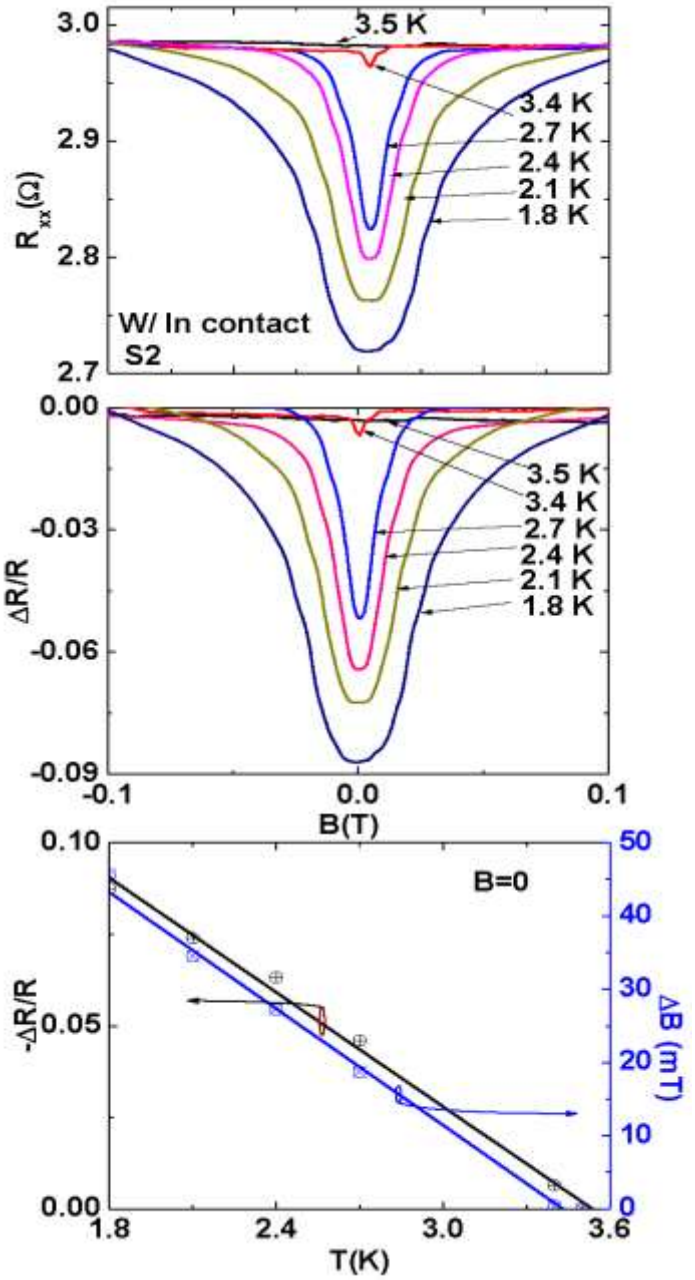

$$2\pi(n + \gamma) = S_F / 2\pi B$$

Fermi surface $S_F = 3.94 \times 10^{17}\ m^{-2}$

$\gamma = 0.41 \pm 0.09$, slightly deviates from exactly π Berry phase

Fractional variation of the magneto resistance ($\Delta R/R$) vs. magnetic field for S2 at different temperature.

$$\frac{\Delta R}{R} = \frac{[R(0.15T) - R(0)]}{R(0.15T)}$$

Variation of R and ΔB measured with respect of 3.5K curve at B=0

Positive resistance correction in GaAs

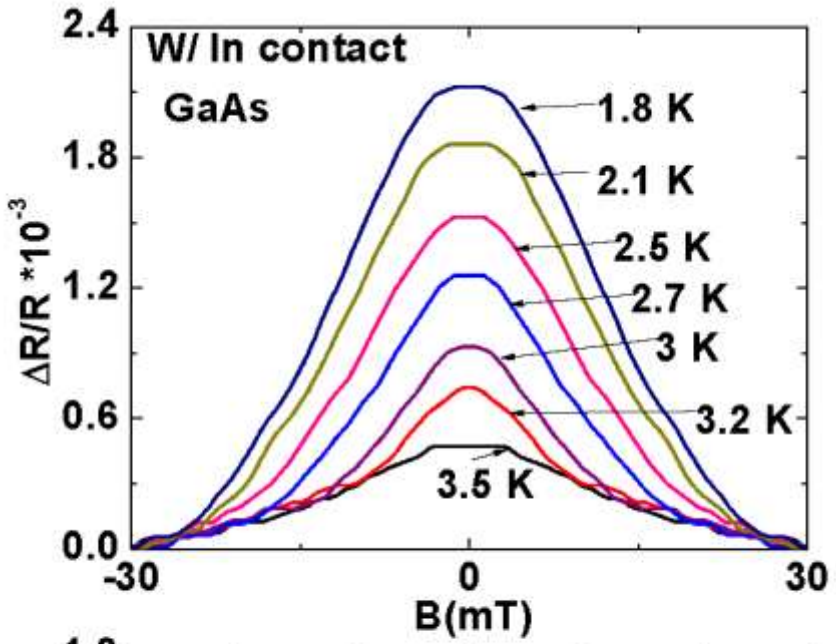

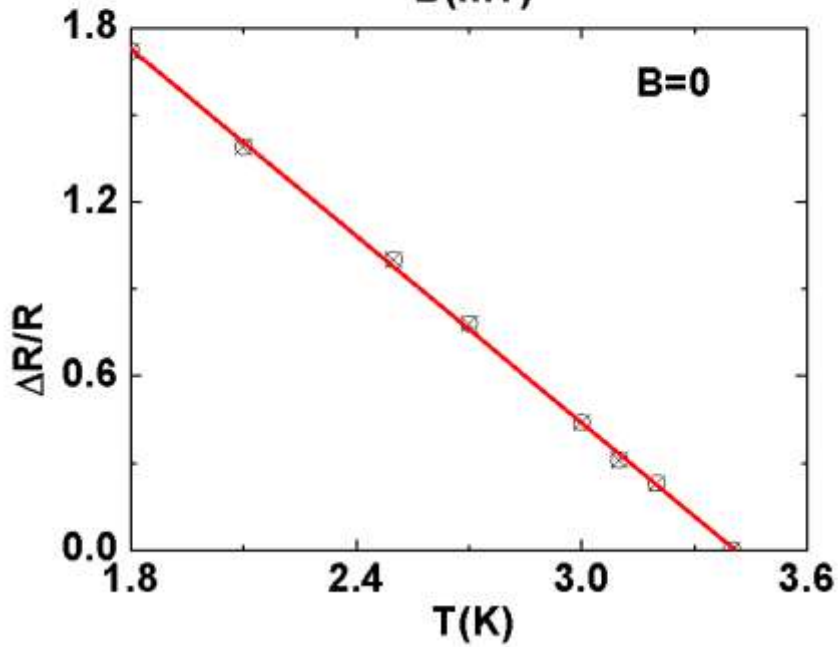

$$\frac{\Delta R}{R} = \frac{[R(30mT) - R(0)]}{R(30mT)}$$

Variation of R measured with respect of 3.5K curve at B=0

R_{xx} plotted vs. magnetic field

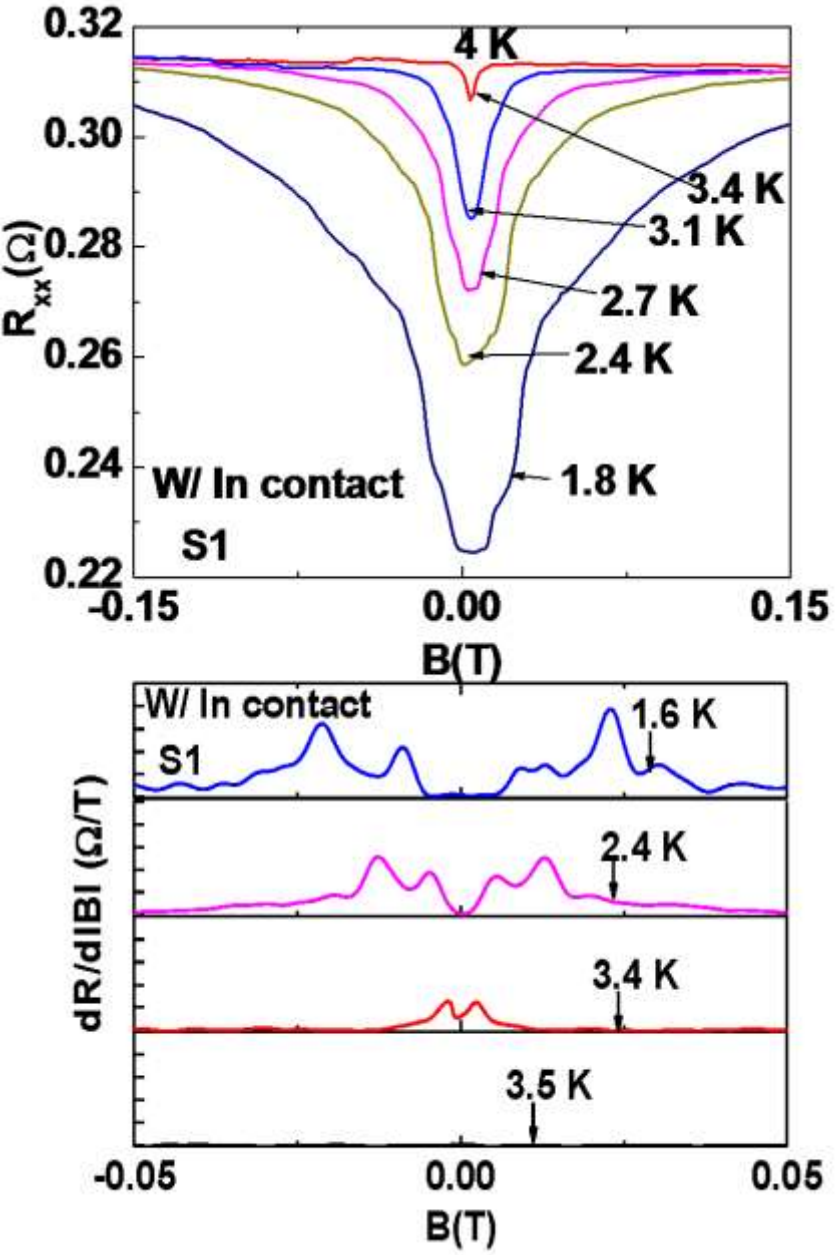

R_{xx} plotted vs magnetic field in temperature range of 3.5 K to 1.8 K ranges in Bi_2Te_3.

dR/d|B|-B plots at various temperatures in vicinity of ±0.05T.

$\Delta B \sim 7$ Oe

$I_s \propto \sin(\Delta\varphi - 4\pi e/hHS)$

HS=magnetic flux through the sample

$\Delta\varphi$= Different in the phases

Conclusions

❖Magnetoresistance measurement were performed on proximity-induced superconducting regions in topological insulator Bi_2Te_3.

❖ Prominent zero field magnetoresistance valley were observed, which were attributed to surface Andreev bound states, possibly related to majorana fermions. Periodic oscillations in different magnetoresistance due to oscillations in the supercurrent in S-N-S junctions, in the presence of magnetic field.

Film Fabrication & its Characterization

RCA cleaning
p-Si substrate

Cleaned p-Si

Thin (50nm) TI film of TI Grown superficially by DC sputtering or Thermal evaporator

Typical process flow depicting fabrication of $Ni_{80}Fe_{20}$/TI/p-Si photodetectors (developed at spintronic and magnetic material laboratory (IIITA)

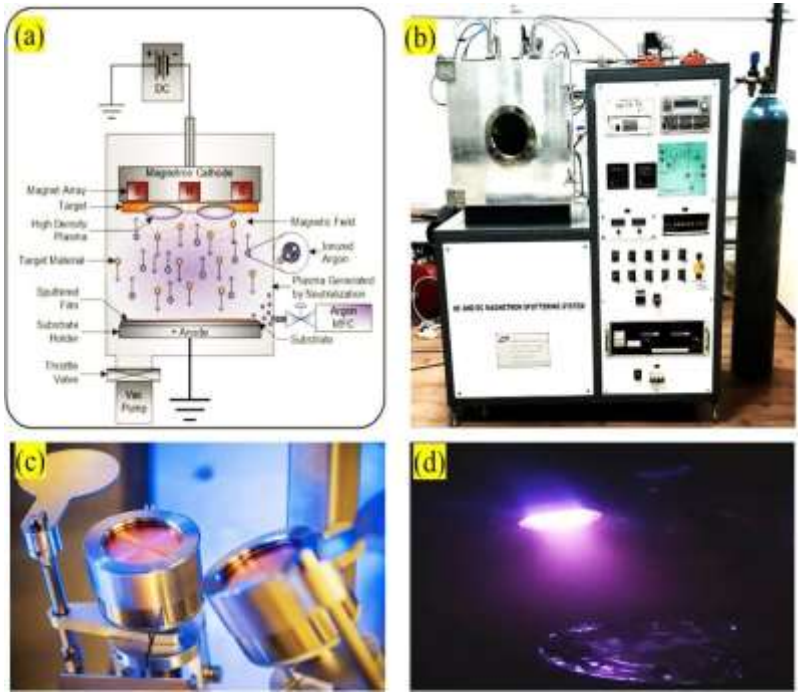

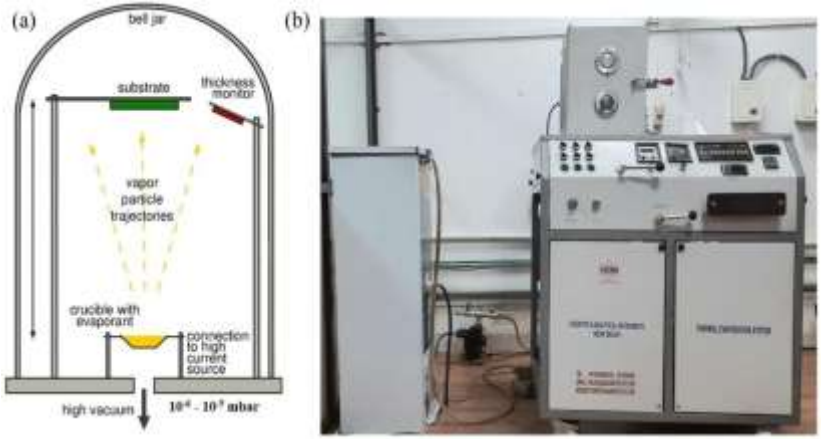

Crucible temperature : 600^0c to 800^0C

Vacuum level: High vacuum or ultra-high vacuum (UHV) to prevent contamination. A pressure of around 10^{-6} to 10^{-7} Torr.
Argon Flow rate : 10 to 50 SCCM

TI Materials prepared: Bi_2Se_3, Bi_2Te_3, Bi_2Te_2Se, $TlBiSe_2$, MoS_2, $MoSe_2$, CrSe, FeSe etc..

1

Thickness depend of TI materials

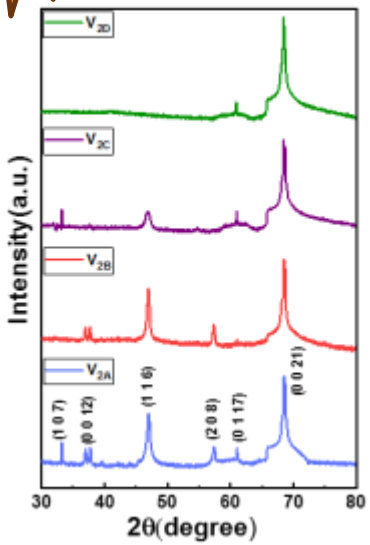

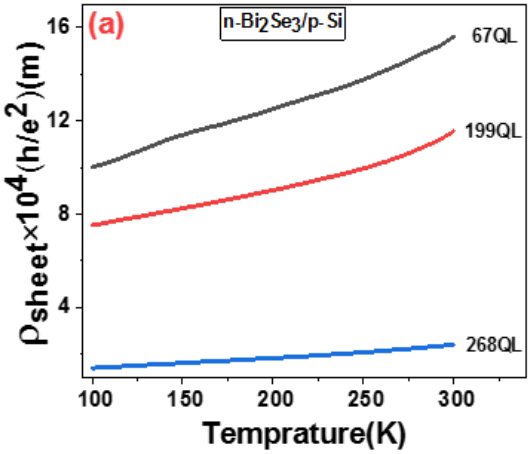

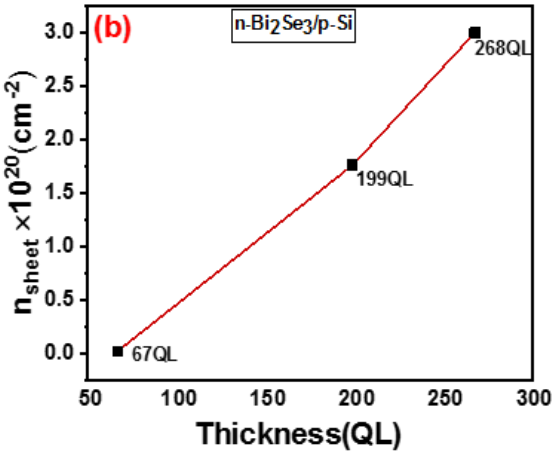

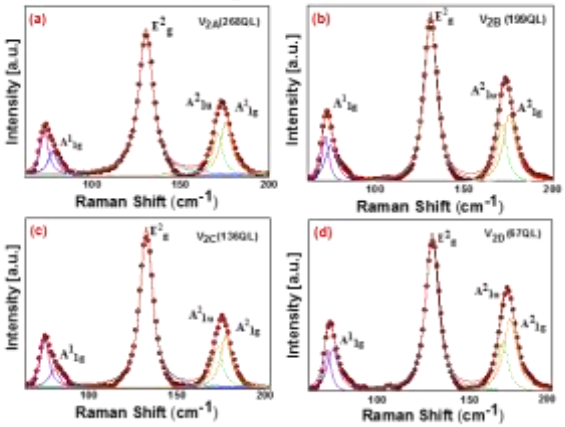

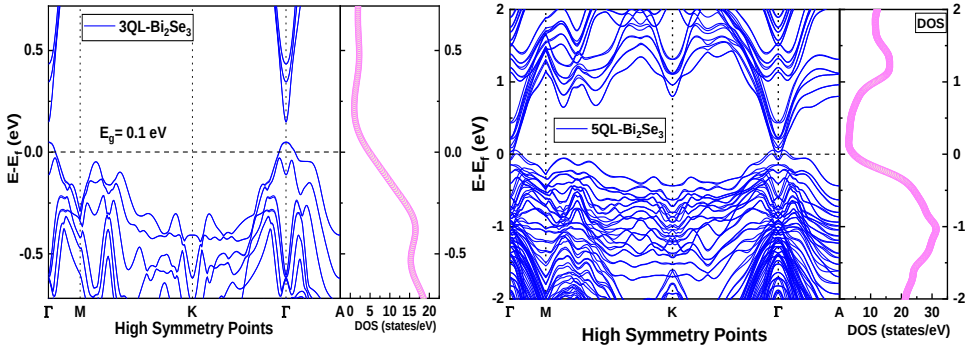

Fig. Band structure and total density of states (DOS) for (a) 3QL (b) 5QL of Bi_2Se_3

Sample	A^1_{1g}(cm^{-1})	E^2_g(cm^{-1})	A^2_{1g}(cm^{-1})	A^2_{1u}(cm^{-1})
V_{2A} (268QL)	72.81	132.65	175.57	171.07
V_{2B} (199QL)	72.53	132.17	175.08	170.57
V_{2C} (136QL)	71.77	133.02	175.39	171.34
V_{2D} (67QL)	72.83	134.00	176.23	172.19

Bulk induced photo-current in topological insulating materials (Bi2Se3/Si) heterojunction for highly responsive photodetectors. Vidushi Gautam et.el.

Device Fabrication & its Characterization

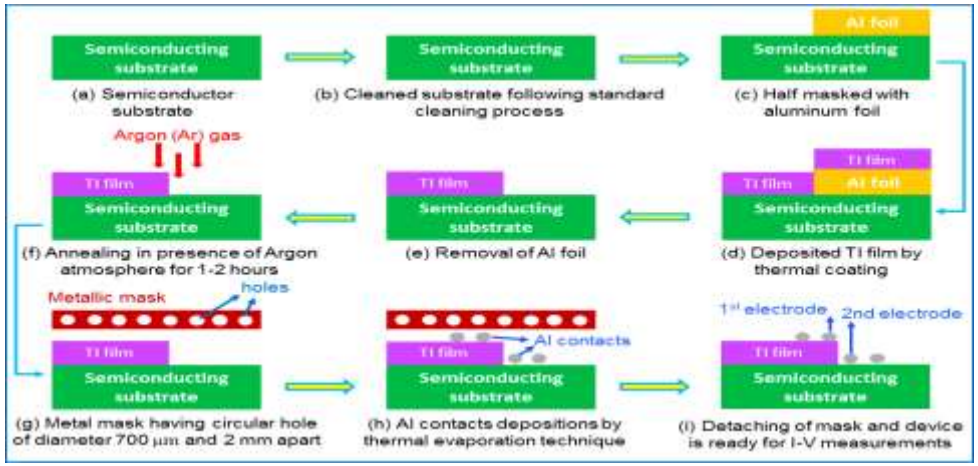

Figure Depicts the flowchart of steps acquired for the fabrication of the TI/semiconductor heterojunction devices

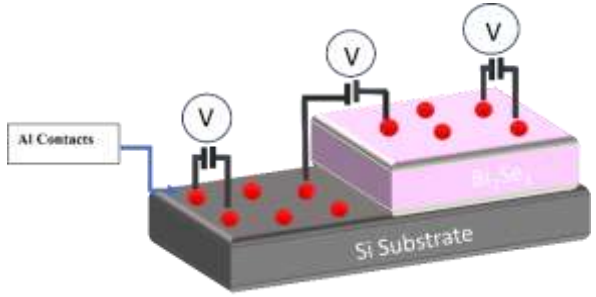

Schematic of fabricated device

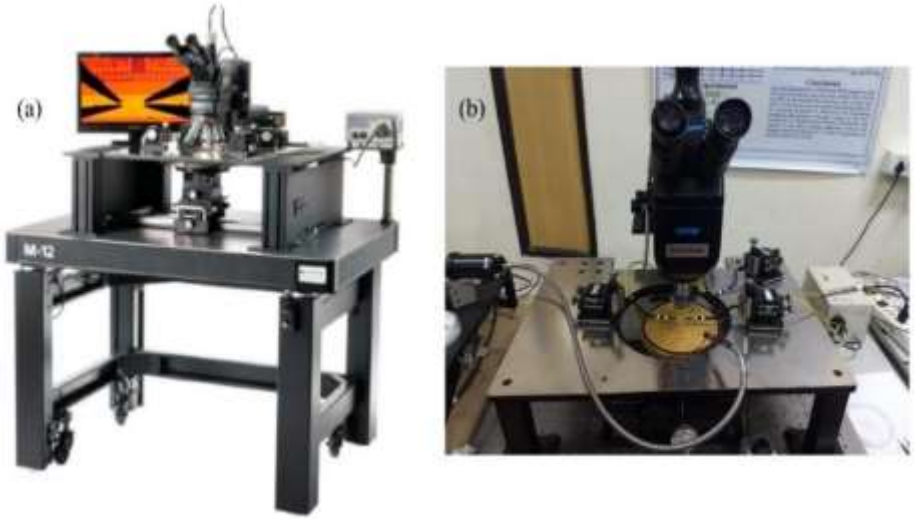

Figure (a) displays the manual probe set up comprising with a 300 mm wafer chuck, a stationary platen with a direct current (DC) source and compound optics.

Figure (a) displays the TLS with a filter having Ozone Free Xe, comprises USB and Interchangeable Slits.

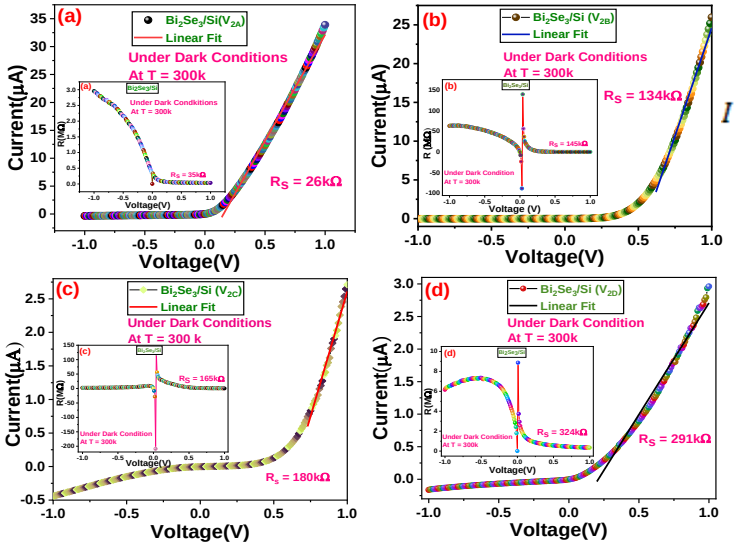

$$I = I_O \left[\exp\left(\frac{qV}{\eta k_B T}\right) - 1\right]$$

$$\eta = \left(\frac{q}{k_B T}\right)\left[\frac{dV}{d(lnI)}\right]$$

$$\frac{dV}{d(lnI)} = \frac{\eta k_B T}{q} + IR_S$$

Fig . Current-Voltage (I-V) measurements of the heterostructure Bi_2Se_3/Si under dark conditions

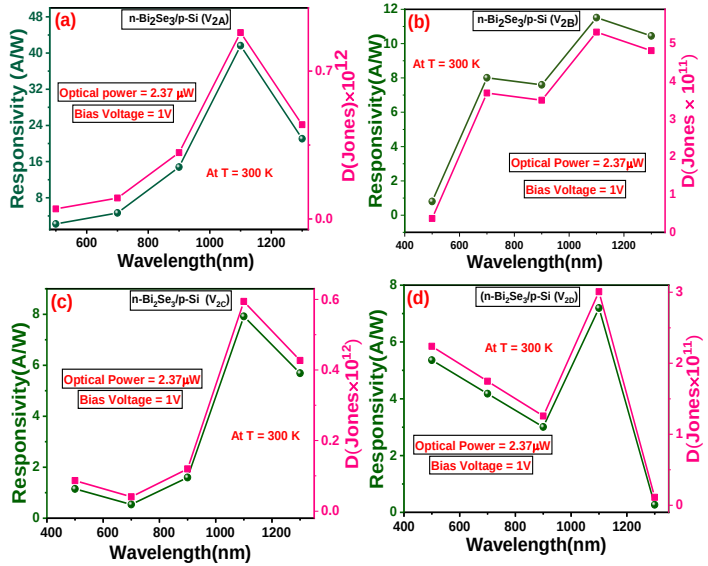

Fig. Responsivity-wavelength (R-λ) curve (Pink) and detective-wavelength (D-λ) plot (green) for Bi_2Se_3/Si heterostructure diode

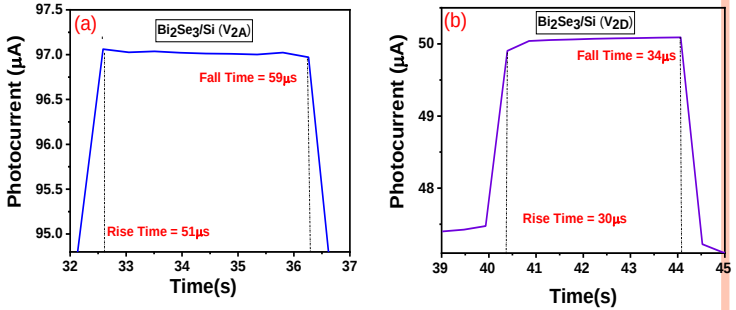

Fig. shows the rise time and decay time for V_{2A} and V_{2D} substrate.

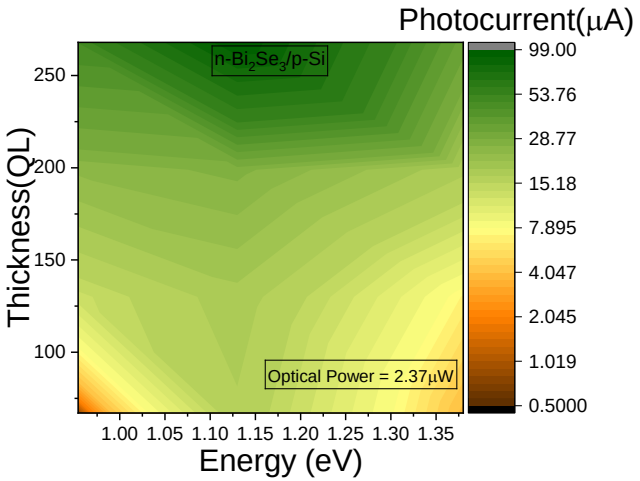

Fig. . Displays the contour relationship between thickness and energy

Responsivity $R = I_{ph}/P_i$

Detectivity $D = RA^{1/2}/\sqrt{2qI_{dark}}$

Photoconductive Gain $G = Rhv/q\eta$

Table : Summary of various parameters of different thicknesses calculated by I-V measurements.

Devices	Ideality factor (η)	Reverse Saturation Current (I_R) in (μA)	Series Resistance (R_S) in KΩ	Maximum Rectification ratio (RR)	$FOM = \gamma . \frac{I_F}{I_R . n . R_S}$
V_{2A}	3.71	0.3	26	100	1.03
V_{2B}	2.47	0.02	134	1624	4.90
V_{2C}	5.31	0.01	180	6.17	0.006
V_{2D}	11.7	0.07	291	18.2	0.005

Table : Summarized parameters determined from optical characteristics

Sample name	Thickness (QL)	R(A/W)	D(Jones)	Photoconductive gain
V_{2A}	268	41.7	0.91×10^{12}	46.9(+1V)
V_{2B}	199	11.5	0.53×10^{12}	12.9(+1V)
V_{2C}	136	7.91	0.59×10^{12}	8.8(+1V)
V_{2D}	67	7.10	0.30×10^{12}	7.9(+1V)

Bulk induced photo-current in topological insulating materials (Bi2Se3/Si) heterojunction for highly responsive photodetectors. Vidushi Gautam et.el.

Challenges in topological electronic devices

- Purity and quality of material
- Stability of Temperature
- Scability and complexity
- Robustness against disorder

Requirement of topological magnetic devices

- Improved stability and control
- Enhanced thermal stability
- Spintronics applications
- Quantum processing of information

2

- **$TlBiSe_2$ was used as a precursor to fabricate a thin film of $TlBiSe_2$ employing the thermal evaporation process (12A40D model manually operated) at room temperature under high vacuum (10-6 Torr).**
- **Then by using sputtering system, in half portion of this film, $Ni_{80}Fe_{20}$ material is deposited to fabricate $Ni_{80}Fe_{20}$/p-$TlBiSe_2$/p-Si heterojunction.**

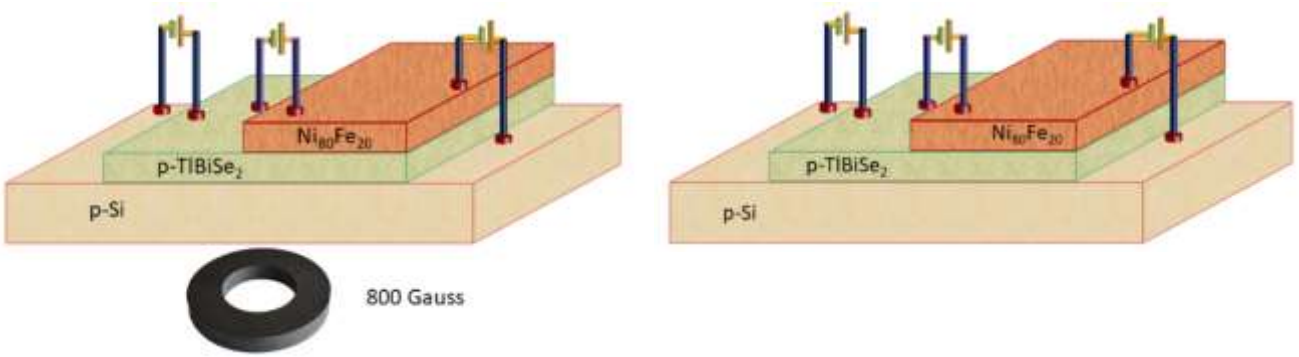

Proximity induced band gap opening in topological magnetic hetero-structure (Ni80Fe20/p-TlBiSe2/p-Si) under ambient condition. (scientific report). Roshani Singh et.al.

.

Raman analysis

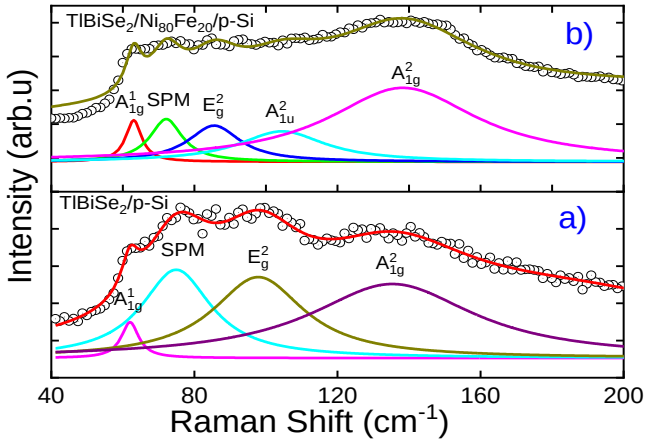

Vibrational modes	p-TlBiSe$_2$/p-Si Peak position (cm^{-1})	FWHM (cm^{-1})	I(A^2_{1g})/I(E^2_g)	p-TlBiSe$_2$/Ni$_{80}$Fe$_{20}$/ p-Si Peak position (cm^{-1})	FWHM (cm^{-1})	I(A^2_{1g})/I(E^2_g)
A^1_{1g}	61.99±0.32	5.92±1.58		63.09±0.44	5.45 ± 1.67	
E^2_g	97.85±0.84	31.10±4.42		85.52±1.68	17.63±10.27	
A^2_{1g}	135.3±1.47	55.95±17.2	1.38	138.32±1.81	50.79± 6.05	1.62
SPM	74.91±0.54	23.70±3.69		72.14±0.84	10.93 ± 4.69	
A^2_{1u}				104.51±3.59	29.16±16.29	

➢ **To determine the life time of each spectra the kinetic profile for each signal is stimulated using the phonon fitting model in the surface xplorer software**

TAS Study

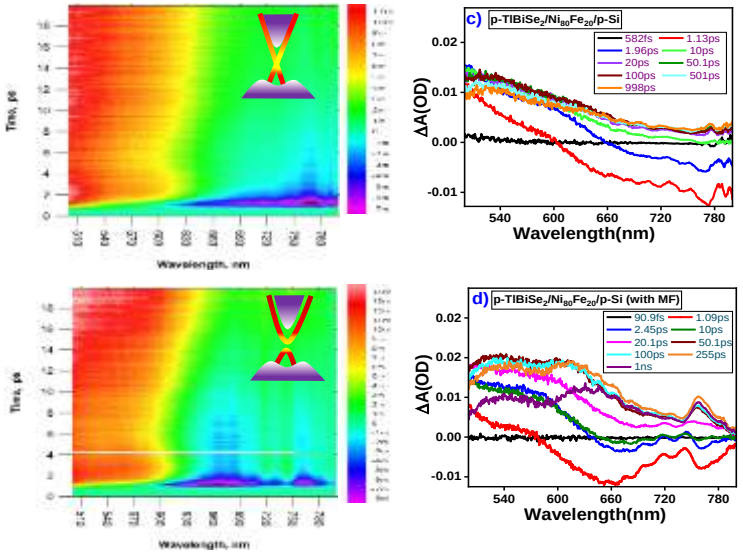

TlBiSe$_2$/Ni$_{80}$Fe$_{20}$ /p-Si (in AMF)				TlBiSe$_2$/Ni$_{80}$Fe$_{20}$ /p-Si (in PMF)			
Wavelength(λ)nm	E(ev)= 1240/ λ	τ_1	τ_2	Wavelength (λ)nm	E(ev) = 1240/ λ	τ_1	τ_2
505 (TA) (1.96 ps)	2.45	257 ps	1.99 ns	505 (TA) (2.45 ps)	2.45	1.4 ps	15.8 ps
615 (GSB) (1.33 ps)	2.02	2.63 ns	2.26 ns	650(GSB) (1.04 ps)	1.91	6.2 ps	708.3 fs
760 (GSB)	1.63	43 ps	6.8 ps	760 (TA)	1.63	1ps	10 ps

$$S(t) = e^{-\left(\frac{t-to}{tp}\right)^2} * \sum_i A_i\, e^{-\frac{t-t0}{ti}}$$

Proximity induced band gap opening in topological magnetic hetero-structure (Ni80Fe20/p-TlBiSe2/p-Si) under ambient condition. (scientific report). Roshani Singh et.al.

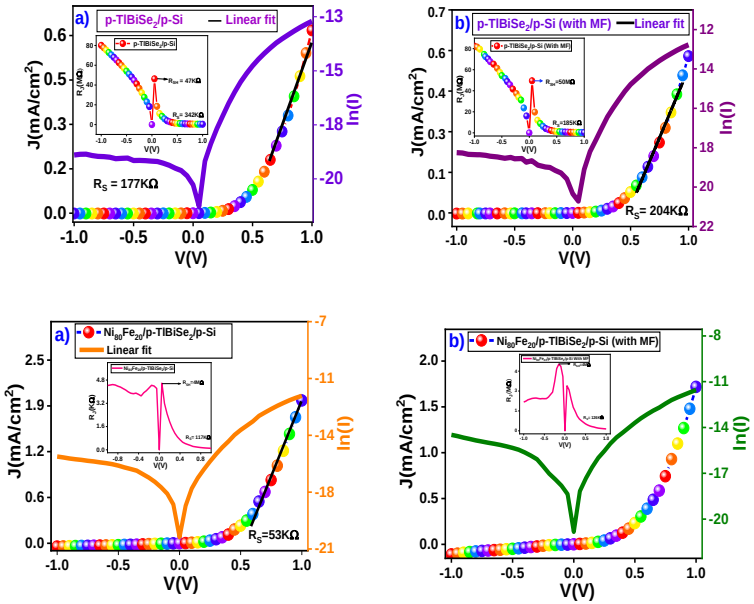

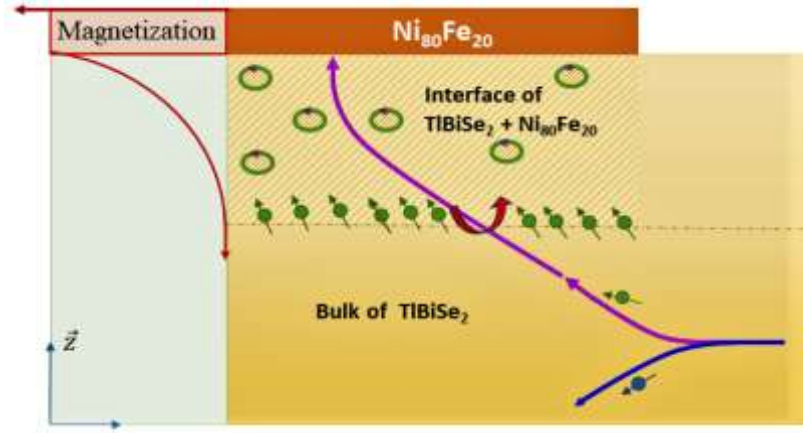

Figure shows Schematic for generation of spin orbit torque (SOT) in $Ni_{80}Fe_{20}$/p-$TlBiSe_2$

Table : Under dark condition the calculated diode parameters

Device	Forward current I_F(μA)	Reverse current I_R (nA)	Rectification Ratio I_F/I_R	R_S (KΩ)	R_{SH} (MΩ)	η from slop of ln(I) vs V plot	η from cheung's method
p-$TlBiSe_2$/p-Si (AMF)	3.03	0.013	245	177	50	4.6	4.4
p-$TlBiSe_2$/p-Si (PMF)	2.1	0.012	239	185	47	4.95	4.8
$Ni_{80}Fe_{20}$/p-$TlBiSe_2$/p-Si (AMF)	9.4	0.23	42	53	85	4	4.3
$Ni_{80}Fe_{20}$/p-$TlBiSe_2$/p-Si (PMF)	8.2	0.53	15	58	80	5.13	5

The conventional diode equation

$$I = I_O \left[\exp\left(\frac{qV}{\eta k_B T}\right) - 1\right]$$

The ideality factor can be obtained from

$$\eta = \left(\frac{q}{k_B T}\right)\left[\frac{dV}{d(lnI)}\right]$$

The Cheung's functions

$$\frac{dV}{d(lnI)} = \frac{\eta k_B T}{q} + IR_S$$

Proximity induced band gap opening in topologcal magnetic hetero-structure (Ni80Fe20/p-TlBiSe2/p-Si) under ambient condition. (scientific report). Roshani Singh et.al.

.

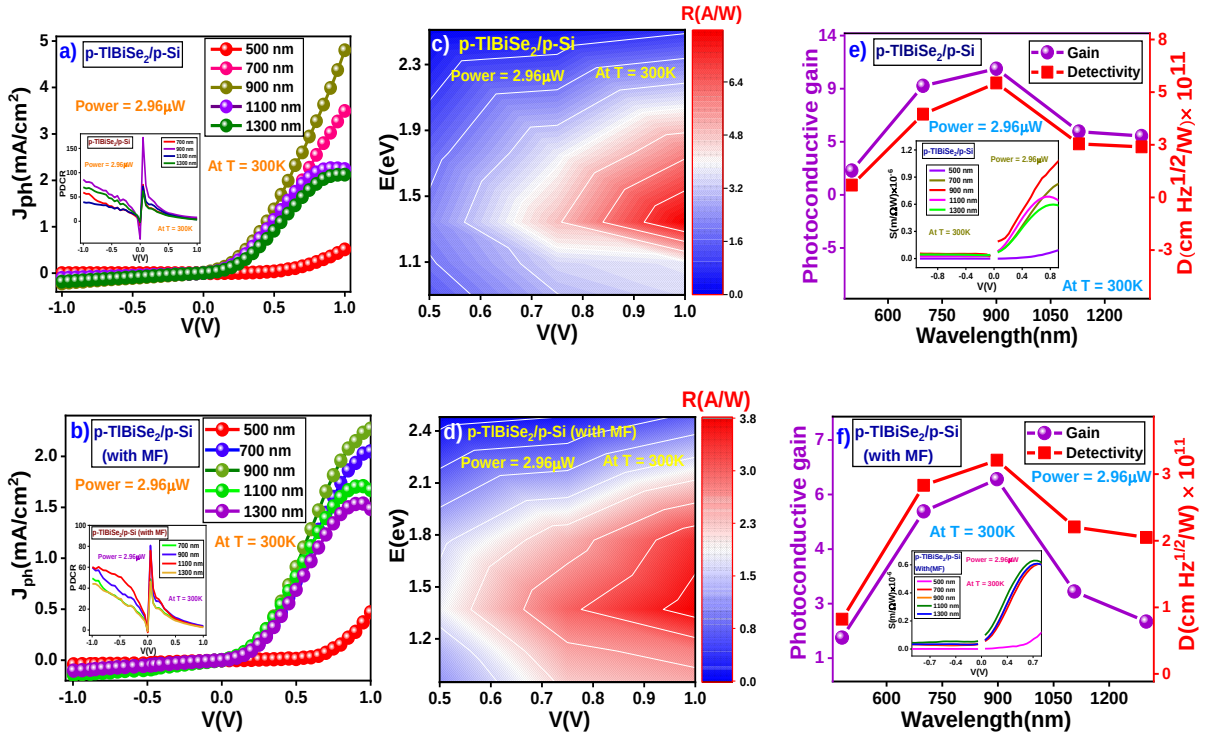

$$PDCR = I_{ph}/I_{dark}$$

$$R = I_{ph}/P_i$$

$$D = RA^{1/2}/\sqrt{2qI_{dark}}$$

$$S = R(d/V_d)$$

$$G = Rhv/q\eta$$

Figure : Optoelectronic characteristics of p-$TlBiSe_2$/p-si heterojunction under varying wavelength from 500 to 1300 nm at 2.96 μW power, in AMF and PMF..

Device	Wavelength (nm)	Forward current (I_F)(μA)	PDCR	R(A/W)	Gain	D(cm Hz1/2/W) ×10^{11}	S (m/ΩW)×10^{-6}
p-$TlBiSe_2$/p-Si (AMF)	900	3	7.74	7.94	10.93	5.65	1.92
p-$TlBiSe_2$/p-Si (PMF)	900	2.27	3.91	3.75	5.78	2.90	0.55
$Ni_{80}Fe_{20}$/p-$TlBiSe_2$ (AMF)	600	411	-	141	290	12.25	-
$Ni_{80}Fe_{20}$/p-$TlBiSe_2$ (PMF)	600	122	-	100	280	9.12	-

Table :List of photo detection parameters at maximum operating wavelength for p-$TlBiSe_2$/p-Si and $Ni_{80}Fe_{20}$/p-$TlBiSe_2$ heterojunction in AMF and PMF.

Proximity induced band gap opening in topologcal magnetic hetero-structure (Ni80Fe20/p-TlBiSe2/p-Si) under ambient condition. (scientific report). Roshani Singh et.al.

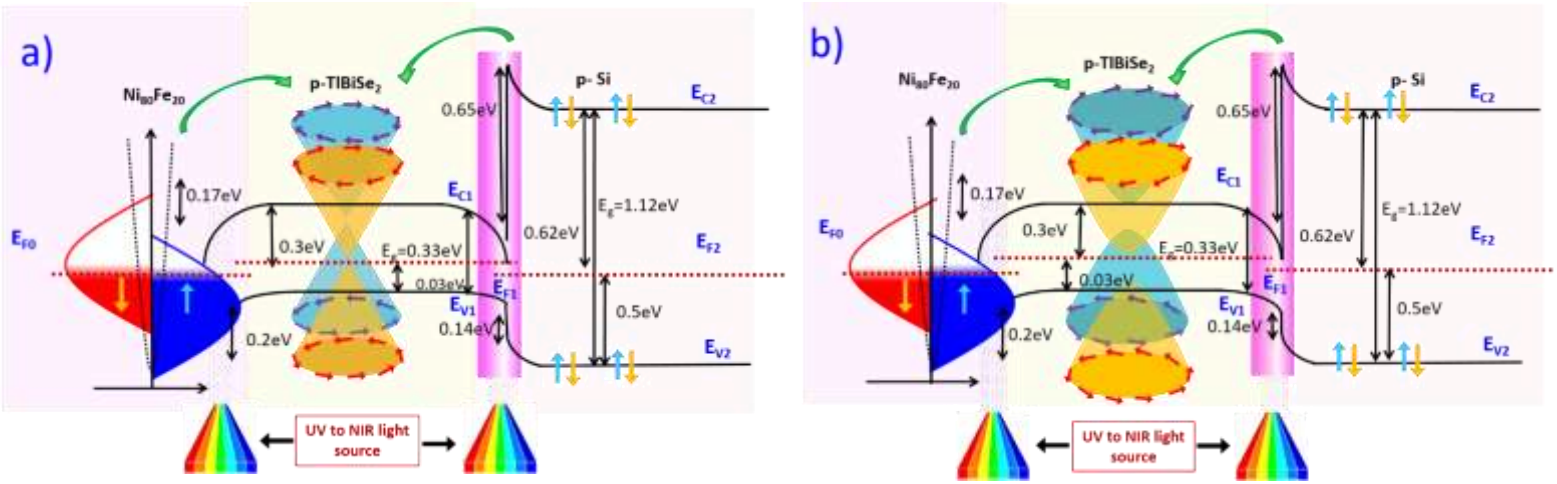

Schematic of the energy band diagram of the $Ni_{80}Fe_{20}$/p-$TlBiSe_2$/p-Si heterostructure in absence and presence of magnetic field

Proximity induced band gap opening in topologcal magnetic hetero-structure (Ni80Fe20/p-TlBiSe2/p-Si) under ambient condition. (scientific report). Roshani Singh et.al.

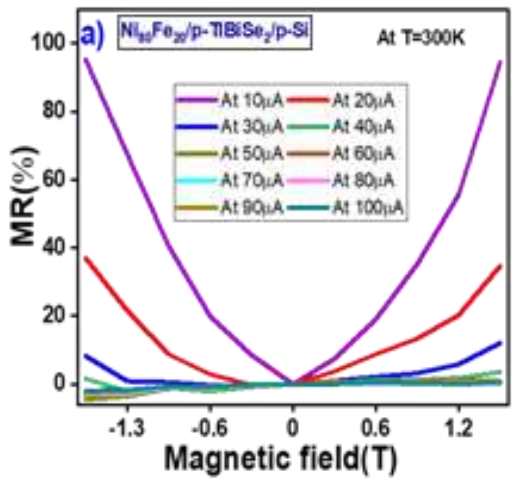

$defined\ as = (R_B - R_0)/R_0] \times 100$

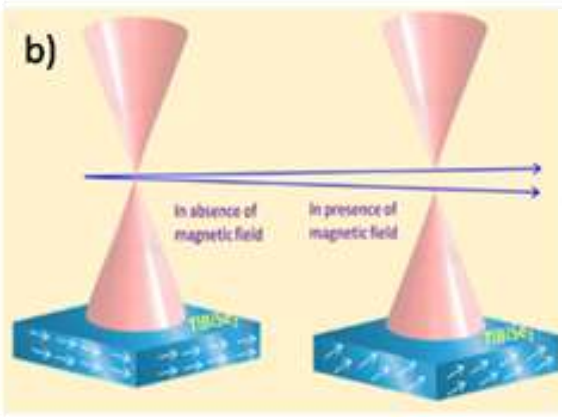

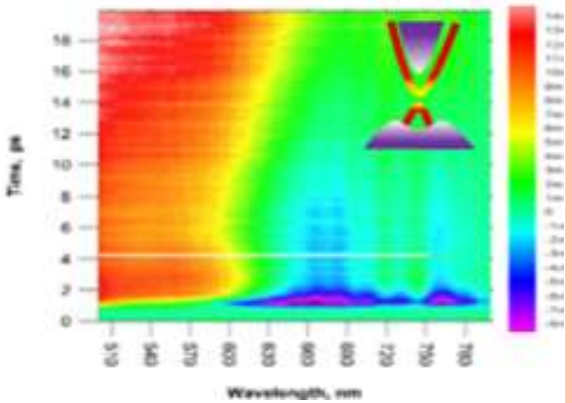

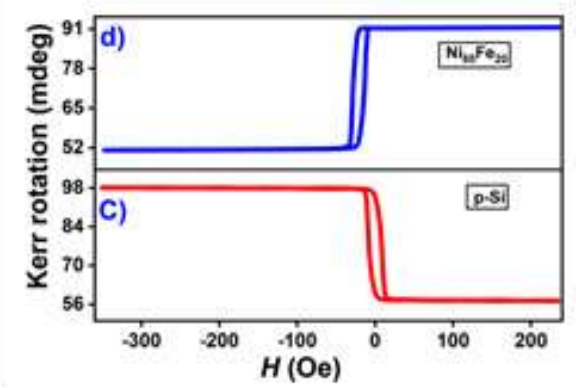

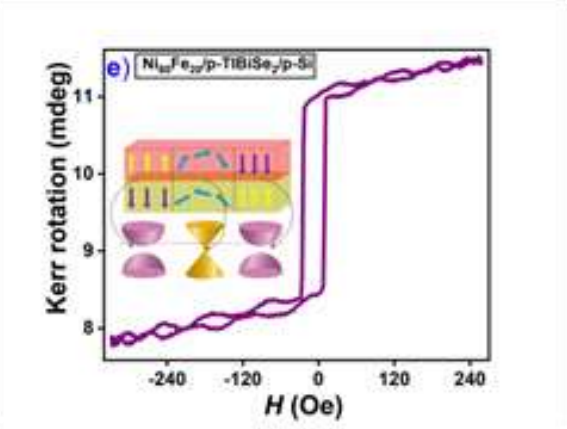

- In TI materials, WAL effect originates due to the strong SOC and spin-momentum locking in the surface states. While in PMF, domination of WL and separation of WAL occur simultaneously. The crossover of WL is a clear evidence of TRS breaking and the appearance of a topological gap in surface states.

Proximity induced band gap opening in topologcal magnetic hetero-structure (Ni80Fe20/p-TlBiSe2/p-Si) under ambient condition. (scientific report). Roshani Singh et.al.

Summary

1

- The Resistivity – temperature analysis also suggests a bulk contribution with increasing quintuple layers.
- The device features a high optoelectronic properties for higher quintuple layer making it superior for optoelectronic applications**.**

2

- The $Ni_{80}Fe_{20}$/TI/Si heterostructure was fabricated using PVD technique and electrical analysis of device under absence and presence of magnetic field was done.
- The diode response under the application of external magnetic field has been decreased.
- TAS study revealed Zeeman splitting of energy levels under a magnetic field, indicating a bandgap at the Dirac point. A bandgap is essential for controlling spin-polarized current and achieving phenomena like the **quantum anomalous Hall effect (QAHE)**.
- MR measurements showed positive magnetoresistance, consistent with increased backscattering due to the bandgap.
- TAS under magnetic fields showed faster carrier relaxation times due to stronger electron-phonon interactions at the interface.
- Faster relaxation improves energy dissipation, making the heterostructure suitable for high-speed spintronic applications.
- This research has significant implications for spintronics. By tuning electronic properties with magnetic fields, we can enhance spin manipulation, paving the way for advanced devices.
- In conclusion, our study highlights how the integration of $Ni_{80}Fe_{20}$ and the application of magnetic fields influence charge carrier dynamics in TIs. We demonstrated TRS breaking, electronic state splitting, and reduced carrier lifetimes, all of which are foundational for spintronic advancements.

Our group and Collaborators

IITB

K.G Suresh

IITH

Arabinda Halder

CSIR-NPL

Sunil Kushwaha

CSIR-IITR

Rachana Kumar

Ph.D. Students

IIITA

Vidushi Gautam

Roshani Singh

S.M.Zaid Ashraf

IMM-CNR, Italy

Claudia Wiemer

Polytechnic University of Marche, Italy.

Arun Kumar

Alumni

Dr. Rashmi Singh
Dr. Faizan Ahmad
Dr. Ankit Singh
Dr. Sanjay Singh
Dr. Pratiksha Shukla
Dr. Gyanendra Kumar Maurya
Dr. Surendra Kumar ……etc

"Thank You and See You at Mahakumbh 2025!"

Quantum Computing Breakthrough Latest News

•Recently, Microsoft announced *Majorana 1*, a new quantum computing chip developed using engineered particles in a new state of matter, which the company sees as a breakthrough.
•With this Microsoft aims to develop quantum computers capable of solving industrial-scale problems within years (2027-29) rather than decades.
•Though, the company has not released any performance data on its quantum chip yet.

Microsoft's Unique Approach to Quantum Computing

For the past 20 years, Microsoft has focused on developing *topological qubits*, which are more stable and require less error correction than traditional qubits.

- Topological qubits are a more stable type of quantum bit, the basic unit of quantum computers.
- They store information in the way specially engineered particles called **anyons** are arranged and braided, not in the particles themselves, making them less prone to errors.
- Anyons are two-dimensional systems. They are neither fermions nor bosons, but have statistical properties in between the two.

Challenges in Creating Topological Qubits

•Developing these qubits posed a steep learning curve, as **Majorana fermions**—particles that are their own antiparticles—had never been physically observed before.

- A Majorana fermion is a hypothetical particle in particle physics that is its own antiparticle, meaning it acts identically to its antiparticle.
- Essentially, it is a fermion that can be considered as its own mirror image, unlike other particles which have distinct antiparticles.

•Although theorized by Ettore Majorana over 80 years ago, evidence of a type known as **Majorana zero modes (MZMs)** has only emerged in the last decade.

- MZM is a special type of quantum state that appears at the ends of certain topological superconductors.
- It is characterized by being its own antiparticle, meaning it acts like both matter and antimatter simultaneously, and exists at zero energy.
- Due to this it becomes a promising candidate for robust quantum computation.

Building a New Quantum Material: Topoconductors

•To fabricate these new particles, Microsoft developed **topoconductors**, made by combining indium arsenide (a semiconductor) and aluminum (a superconductor).

- Just as semiconductors enabled modern electronics, topoconductors pave the way for scalable quantum systems, potentially reaching a million qubits to solve complex industrial and societal challenges.

•When cooled to near absolute zero and exposed to magnetic fields, these materials merge superconductivity with semiconductors, enabling the creation of a new type of qubit.

Majorana 1

•Microsoft's *Majorana 1* is an ***eight-qubit*** **chip**, which is modest compared to rivals like Google's *Willow (106 qubits)* and IBM's *R2 Heron (156 qubits)*.

•However, its *Topological Core* architecture could allow scaling up to a *million qubits*, a necessary threshold for solving real-world problems.

Majorana 1's Design

•Microsoft's Majorana 1 chip features aluminum nanowires arranged in an "H" shape.

•Each "H" structure has four controllable Majorana particles, forming a single qubit.

Potential Applications of Quantum Computing

•Microsoft envisions Majorana 1 helping to develop breakthroughs such as:

- Breaking down *microplastics* into harmless byproducts.
- Inventing *self-healing materials* for construction, manufacturing, and healthcare.

•Microsoft envisions using quantum computing with generative AI to design new materials or molecules through natural language input.

•Quantum computing could generate synthetic data to improve AI model training.

Challenges

•Quantum systems are highly sensitive to environmental interference, causing errors.

Quantum Computers vs Supercomputers vs Classical Computers

- **Classical Computers**
  - Classical computers process information using binary code (bits) with values of either 0 or 1.
  - They rely on logic gates (AND, OR, XOR, NOT) to manipulate data.
- **Quantum Computers**
  - Quantum computers use qubits, which can exist in multiple states simultaneously (superposition).
  - A qubit can have probabilities assigned to both 0 and 1, allowing it to store and process more information than a classical bit.
  - Quantum gates (H-gate, Pauli gates) enable the processing of qubits and are reversible in nature.
- **Supercomputers**
  - Supercomputers use advanced architectures with GPUs and multi-core processing to perform calculations faster than regular computers.
  - Despite their power, they still follow classical computing principles and logic gates.
- **Quantum vs. Supercomputers**
  - While supercomputers enhance classical processing speed, quantum computers can solve complex problems that classical and supercomputers cannot.
  - Quantum gates enable unique computational abilities beyond traditional logic gates.